# 🧠R2I-Bench: Benchmarking Reasoning-Driven Text-to-Image Generation

**Kaijie Chen♠, Zihao Lin∗♠, Zhiyang Xu∗♣, Ying Shen∗♦,**
**Yuguang Yao♡, Joy Rimchala♡, Jiaxin Zhang†★, Lifu Huang♠✉**

♠University of California, Davis  ♣Virginia Tech  ♦University of Illinois Urbana-Champaign
♡Intuit AI Research  ★Salesforce AI Research
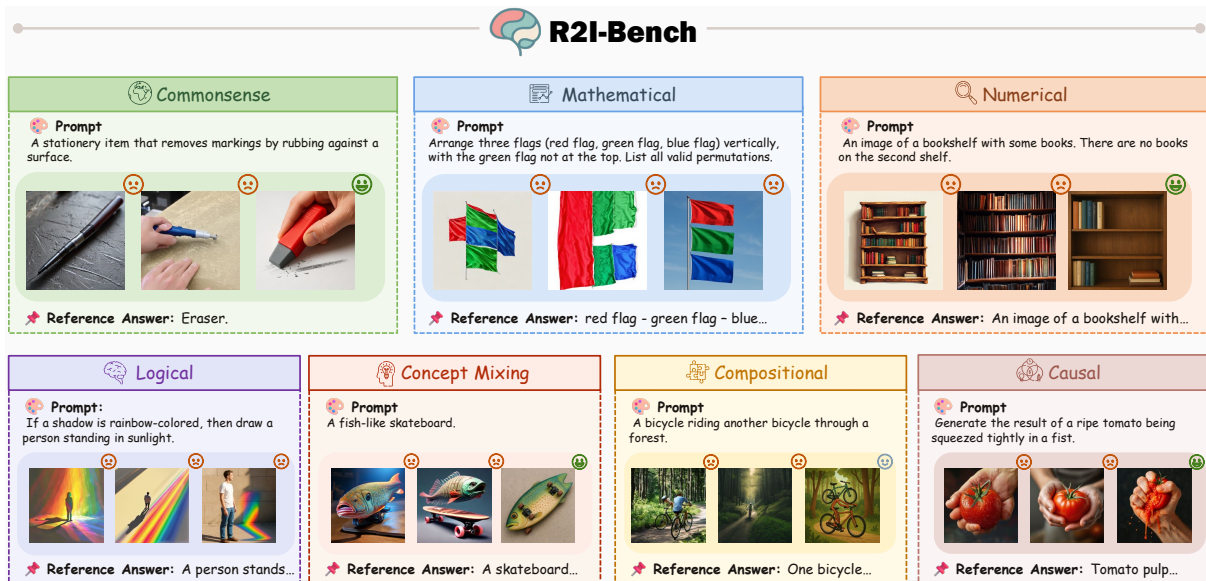jkkjjj715@gmail.com,  lfuhuang@ucdavis.edu

Figure 1: We introduce R2I-Bench, a comprehensive benchmark designed to assess the reasoning capabilities of text-to-image (T2I) generation models. It encompasses 7 primary reasoning categories, which are further subdivided into 32 fine-grained subcategories.

## Abstract

Reasoning is a fundamental capability often required in real-world text-to-image (T2I) generation, e.g., generating "*a bitten apple that has been left in the air for more than a week*" necessitates understanding temporal decay and commonsense concepts. While recent T2I models have made impressive progress in producing photorealistic images, their reasoning capability remains underdeveloped and insufficiently evaluated. To bridge this gap, we introduce R2I-Bench, a comprehensive benchmark specifically designed to rigorously assess reasoning-driven T2I generation. R2I-Bench comprises 3,068 meticulously curated data instances, spanning 7 core reasoning categories, including commonsense, mathematical, logical, compositional, numerical, causal, and concept mixing. To facilitate fine-grained evaluation, we design R2I-Score, a QA-style metric based on instance-specific, reasoning-oriented evaluation questions that assess three critical dimensions: *text-image alignment*, *reasoning accuracy*, and *image quality*. Extensive experiments with 17 representative T2I models, including a strong pipeline-based framework that decouples reasoning and generation using the state-of-the-art language and image generation models, demonstrate consistently limited reasoning performance, highlighting the need for more robust, reasoning-aware architectures in the next generation of T2I systems. Project page: https://r2i-bench.github.io.

## 1 Introduction

Reasoning is a fundamental capability underpinning most, if not all, human cognitive tasks, including text-to-image (T2I) generation. In real-world scenarios, prompts often require models to go beyond surface-level descriptions and engage in multi-step reasoning. For example, generating an image for "*a bitten apple that has been left in the*

---

12595

| Benchmarks | Reasoning Capabilities Evaluated in Text-to-Image Generation | | | | | | | Human Annotation |
|---|---|---|---|---|---|---|---|---|
| | Commonsense | Compositional | Numerical | Mathematical | Concept Mixing | Logical | Causal | |
| OK-VQA (Marino et al., 2019) | ✓ | ✗ | ✗ | ✗ | ✗ | ✗ | ✗ | ✗ |
| Winoground (Thrush et al., 2022) | ✗ | ✓ | ✗ | ✗ | ✗ | ✗ | ✗ | ✗ |
| HEIM (Lee et al., 2023) | ✗ | ✓ | ✗ | ✗ | ✗ | ✗ | ✗ | ✗ |
| GeckoNum (Ghosh et al., 2023) | ✗ | ✗ | ✓ | ✗ | ✗ | ✗ | ✗ | ✓ |
| GenEval (Ghosh et al., 2023) | ✗ | ✓ | ✓ | ✗ | ✗ | ✗ | ✗ | ✗ |
| GenAI-Bench (Li et al., 2024) | ✗ | ✗ | ✓ | ✗ | ✗ | ✗ | ✗ | ✗ |
| ConceptMix (Wu et al., 2024) | ✗ | ✓ | ✗ | ✗ | ✓ | ✗ | ✗ | ✗ |
| Commonsense-T2I (Fu et al., 2024) | ✓ | ✗ | ✗ | ✗ | ✗ | ✗ | ✗ | ✗ |
| WISE (Niu et al., 2025) | ✓ | ✗ | ✗ | ✗ | ✗ | ✗ | ✗ | ✗ |
| R2I-Bench (Ours) | ✓ | ✓ | ✓ | ✓ | ✓ | ✓ | ✓ | ✓ |

Table 1: **Comparison between R2I-Bench and existing text-to-image benchmarks.** R2I-Bench covers a broader spectrum of essential reasoning capabilities for text-to-image generation. In addition, R2I-Bench provides manually curated, high-quality evaluation criteria to support rigorous and consistent assessment.

*air for more than a week*" requires understanding the concept of decay over time, inferring the visual appearance of a spoiled apple, composing that with contextual cues, and finally generating an image to depict "*a bitten and spoiled apple*".

However, despite recent advances, most existing T2I models, whether based on diffusion (Esser et al., 2024; Xie et al., 2025a; Qin et al., 2025; Yang et al., 2023), autoregressive transformer (Sun et al., 2024a; Zhang et al., 2024; Chen et al., 2025; Wang et al., 2024; Chen et al., 2024), or unified architectures(Xiao et al., 2024; Xie et al., 2025b; Zhou et al., 2025; Tong et al., 2024; Sun et al., 2023, 2024b), primarily focus on *semantic rendering*, where the prompt explicitly specifies what to generate and the model simply converts it into an image. Although recent work (Jiang et al., 2025; Zhang et al., 2025; Liao et al., 2025) has begun to benchmark and enhance reasoning-driven T2I generation, they are often limited to narrow domains such as commonsense (Niu et al., 2025), numerical reasoning (Ghosh et al., 2023), or concept mixing (Wu et al., 2024). Furthermore, widely adopted evaluation metrics for T2I generation, such as CLIPScore (Hessel et al., 2021), VQAScore (Lin et al., 2024), and WIScore (Niu et al., 2025), mainly assess the semantic alignment between generated images and prompts or fail to generalize across diverse reasoning types, limiting meaningful development, comparison, and assessment of the underlying reasoning capabilities in T2I generation models.

To bridge these gaps, we introduce R2I-Bench (**R**easoning-**to**-**I**mage **Bench**mark), a comprehensive benchmark consisting of 3, 068 meticulously curated text prompts, specifically designed to evaluate the reasoning capabilities of T2I models. Each prompt is initially generated using a state-of-the-art

large language model (i.e., GPT-4o) and subsequently validated and refined by domain experts to ensure the quality and reliability. As shown in Figure 1, R2I-Bench encompasses 7 core reasoning categories, including ***commonsense***, ***compositional***, ***logical***, ***mathematical***, ***causal***, ***numerical***, and ***concept mixing***, which are further subdivided into 32 fine-grained reasoning subcategories. In contrast to prior T2I evaluation datasets, R2I-Bench offers significantly broader and more systematic coverage of diverse reasoning skills, as summarized in Table 1.

To enable fine-grained evaluation of reasoning-driven T2I generation, each T2I prompt in R2I-Bench is paired with a set of instance-specific diagnostic questions and corresponding scoring criteria, all verified by human experts. These questions assess the quality of T2I generation along three critical aspects: (1) text-image alignment, (2) reasoning accuracy, and (3) image quality. Building on these evaluation questions and criteria, we introduce a QA-style metric, R2I-Score, which aggregates scores using a weighted scheme. R2I-Score demonstrates strong alignment with human judgments, offering a more faithful and interpretable performance measure of T2I models on R2I-Bench.

We systematically evaluate 17 representative T2I models on R2I-Bench, spanning diffusion-based, autoregressive, reasoning-enhanced, and closed-source models. To further explore the upper bound of reasoning-driven T2I generation, we also develop a strong pipeline-based framework that decouples reasoning and generation: a state-of-the-art LLM (GPT-4o) first performs reasoning over the prompt and rewrites it into a detailed description, which is then rendered by a high-performing T2I model (SD3-medium). Experimental results re-

veal several key insights: **(1)** All the open-source models achieve less than $45\%$ accuracy, demonstrating limited reasoning capabilities in existing T2I models and underscoring the significance of `R2I-Bench` as a rigorous evaluation benchmark. Notably, these models tend to interpret prompts as bags of words, e.g., they generate both objects for the prompt "*either a spoon or a bowl*", disregarding the logical disjunction; **(2)** Mathematical reasoning remains a persistent challenge across all models, largely due to the lack of diverse, high-quality training data grounded in mathematical concepts and their visual representations; **(3)** Recent efforts to enhance reasoning through Chain of Thought (CoT) or Reinforcement Learning (RL) (Zhang et al., 2025; Liao et al., 2025; Jiang et al., 2025) yield marginal improvements, highlighting the need for more robust, fundamentally reasoning-aware T2I models; and **(4)** While the pipeline-based framework improves performance, it still struggles with abstract mathematical reasoning and accurately interpreting specific linguistic constructs such as quantities, limiters, and quantifiers. Finally, we also conduct a comprehensive qualitative error analysis, categorizing model failures into three main categories, including reasoning errors, visual element errors, and image quality degradation, providing valuable insights to future research.

Our contributions are summarized as follows: (1) We introduce `R2I-Bench`, the first comprehensive benchmark specifically designed to evaluate reasoning-driven T2I generation. Covering a broad range of reasoning categories and meticulously curated through a rigorous human-in-the-loop process, `R2I-Bench` offers a valuable resource for benchmarking and advancing T2I models. (2) To enable fine-grained evaluation of reasoning-driven T2I generation, we design a new metric, `R2I-Score`, built on human-validated evaluation questions and scoring criteria tailored to each data instance in `R2I-Bench`. `R2I-Score` assesses model performance across three critical dimensions, including text-image alignment, reasoning accuracy, and image quality. (3) Through extensive experiments and analysis, we identify several key limitations in all the existing T2I models and provide valuable insights for future research.

## 2 Related Work

**Text-to-Image Generation Models** Recent advances in text-to-image (T2I) generation have pro-

duced high-quality models across various architectures, including diffusion (Esser et al., 2024; Gao et al., 2025; Xie et al., 2025a; Qin et al., 2025; Yang et al., 2023), autoregressive (Sun et al., 2024a; Zhang et al., 2024; Chen et al., 2025; Wang et al., 2024; Qi et al., 2025), and unified frameworks (Xiao et al., 2024; Xie et al., 2025b; Zhou et al., 2025; Tong et al., 2024; Sun et al., 2023, 2024b; Shen et al., 2025; Xu et al., 2025; Xu et al.). More recently, reasoning-augmented models have incorporated chain-of-thought (CoT) reasoning (Liao et al., 2025) and reinforcement learning (Zhang et al., 2025; Jiang et al., 2025) to better handle complex prompts. However, their reasoning capability remains underdeveloped and insufficiently evaluated.

**Text-to-Image Evaluation Benchmarks and Metrics** Existing T2I benchmarks evaluate isolated reasoning skills but lack comprehensive coverage. OK-VQA (Marino et al., 2019), WISE (Niu et al., 2025), Commonsense T2I (Fu et al., 2024) and Visual Riddles (Bitton-Guetta et al., 2024) emphasize shallow or knowledge-based reasoning, while GeckoNum (Kajić et al., 2024) focuses solely on numerical tasks. Benchmarks like Winoground (Thrush et al., 2022), GenEval (Ghosh et al., 2023), and GenAI-Bench (Li et al., 2024) target compositionally. Despite progress, no existing benchmark offers a unified framework for evaluating the full spectrum of T2I reasoning abilities (see Table 1). Current evaluation metrics also lack reasoning sensitivity. CLIPScore (Hessel et al., 2021), DSGScore (Cho et al., 2024), and VQAScore (Lin et al., 2024) underperform on complex reasoning and struggle with compositional or numerical fidelity. LLM-based metrics such as LLM-Score (Lu et al., 2023) and SemVarEffect (Zhu et al., 2025) overlook spatial or relational accuracy. While RIScore (Zhao et al., 2025) and WIScore (Niu et al., 2025) offer GPT-based scoring, they lack the granularity needed for fine-grained evaluation. Thus, a critical gap remains in metrics that rigorously assess reasoning in T2I generation.

## 3 R2I-Bench

**Overview** As shown in the top left part of Figure 2, each data instance in `R2I-Bench` consists of four elements: (1) a reasoning-based T2I prompt which serves as a textual input to the T2I models; (2) a reference caption that explicitly describes the content of the image that is supposed to be
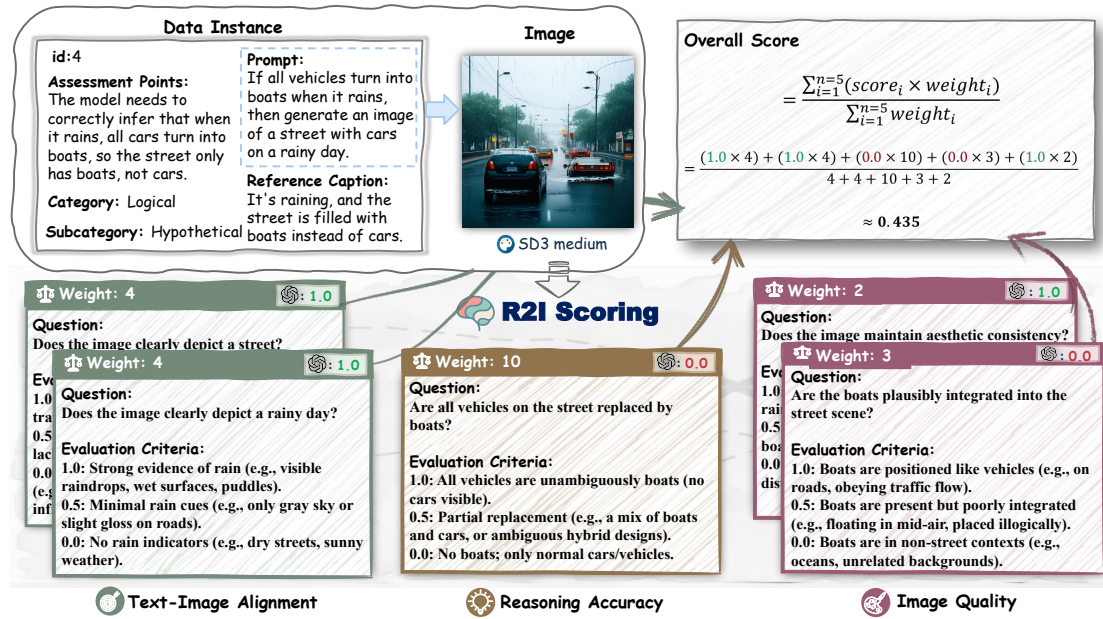
**Data Instance**

id:4

Assessment Points: The model needs to correctly infer that when it rains, all cars turn into boats, so the street only has boats, not cars.

Category: Logical

Subcategory: Hypothetical

Prompt: If all vehicles turn into boats when it rains, then generate an image of a street with cars on a rainy day.

Reference Caption: It's raining, and the street is filled with boats instead of cars.

**Image**

SD3 medium

**Overall Score**

$$= \frac{\sum_{i=1}^{n=5}(score_i \times weight_i)}{\sum_{i=1}^{n=5} weight_i}$$

$$= \frac{(1.0 \times 4) + (1.0 \times 4) + (0.0 \times 10) + (0.0 \times 3) + (1.0 \times 2)}{4 + 4 + 10 + 3 + 2}$$

$$\approx 0.435$$

**R2I Scoring**

Weight: 4 — : 1.0
Question: Does the image clearly depict a street?

Weight: 4 — : 1.0
Question: Does the image clearly depict a rainy day?
Evaluation Criteria:
1.0: Strong evidence of rain (e.g., visible raindrops, wet surfaces, puddles).
0.5: Minimal rain cues (e.g., only gray sky or slight gloss on roads).
0.0: No rain indicators (e.g., dry streets, sunny weather).

Weight: 10 — : 0.0
Question: Are all vehicles on the street replaced by boats?
Evaluation Criteria:
1.0: All vehicles are unambiguously boats (no cars visible).
0.5: Partial replacement (e.g., a mix of boats and cars, or ambiguous hybrid designs).
0.0: No boats; only normal cars/vehicles.

Weight: 2 — : 1.0
Question: Does the image maintain aesthetic consistency?

Weight: 3 — : 0.0
Question: Are the boats plausibly integrated into the street scene?
Evaluation Criteria:
1.0: Boats are positioned like vehicles (e.g., on roads, obeying traffic flow).
0.5: Boats are present but poorly integrated (e.g., floating in mid-air, placed illogically).
0.0: Boats are in non-street contexts (e.g., oceans, unrelated backgrounds).

Text-Image Alignment — Reasoning Accuracy — Image Quality

Figure 2: Example Illustration of `R2I-Bench` and `R2I-Score`.

generated; (3) an explanation description, which explains the reasoning steps from the T2I prompt to the reference caption and is used to generate reasoning-driven evaluation questions; and (4) the category, the subcategory, and the index of the data instance. As illustrated in Appendix A.1 Figure 4, we adopt a human-in-the-loop pipeline to construct `R2I-Bench`, which comprises three main stages: (1) data collection, (2) data filtering, and (3) evaluation criteria generation.

**Data Collection**  We build a human-in-the-loop data generation pipeline as illustrated in Figure 4. In the initial stage, a team of five human experts systematically reviews prior work relevant to text-to-image (T2I) reasoning tasks (Wu et al., 2024; Kajić et al., 2024; Thrush et al., 2022; Li et al., 2024; Liu et al., 2020; Liew et al., 2022; Fu et al., 2024; Chevalley et al., 2022; Niu et al., 2025; Lee et al., 2023). Based on this comprehensive analysis, they identify 7 core reasoning categories frequently required across diverse T2I scenarios: *commonsense*, *compositional*, *logical*, *concept-mixing*, *numerical*, *mathematical*, and *causal reasoning*. These primary categories are further refined into 32 fine-grained subcategories, as illustrated in Figure 3. Detailed definitions for all the core and fine-grained reasoning categories are provided in Appendix A.2.

For each subcategory, we instruct GPT-4o to generate 100-120 T2I prompts designed to test the corresponding reasoning skill, accompanied by reference captions for subsequent evaluation.
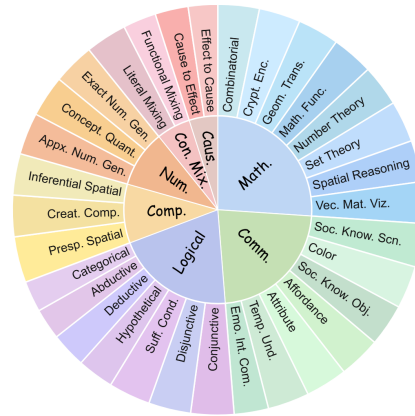
Figure 3: **Distribution of Diverse Reasoning Categories in `R2I-Bench`.** Caus.: Causal. Con. Mix.: Concept Mixing. Math.: Mathematical. Comm.: Commonsense. Num.: Numerical. Comp.: Compositional.

To ensure that the prompts emphasize reasoning and avoid direct visual descriptions, the generation instruction is constrained by two key guidelines: (1) prompts must not explicitly reveal the answer or directly describe visual features, and (2) the corresponding visual elements must be uniquely identifiable. In-context learning is used, where the model is conditioned on three positive and three negative exemplar prompts authored by human experts[1]. For each T2I prompt, we further instruct GPT-4o to generate an explanation describing the necessary reasoning steps based on the corresponding refer-

---

[1] Appendix A.2 presents detailed categories of negative examples in reasoning-driven T2I generation.
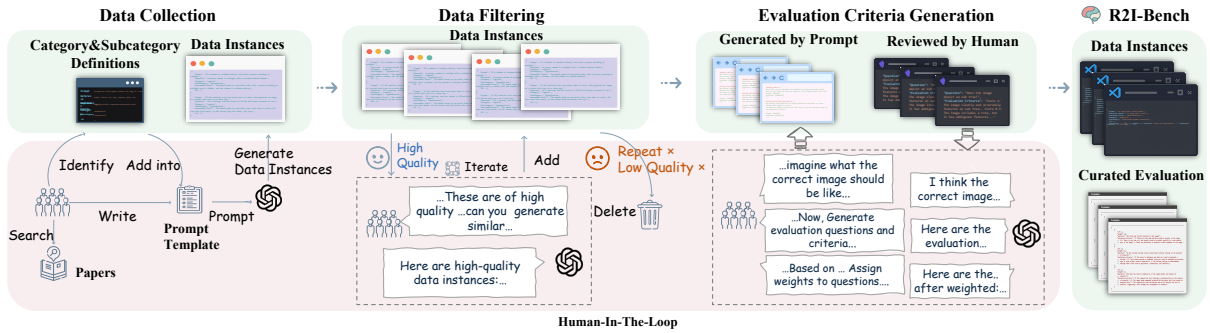
Figure 4: **Benchmark Curation Pipeline.** The pipeline starts with data collection, followed by data filtering, evaluation criteria generation, and ultimately results in `R2I-Bench`. To ensure data quality, human verification is performed at each key stage to eliminate low-quality data, annotations, and ambiguous evaluation questions.

ence caption. The instructions for generating the T2I prompt and explanation description are shown in Appendix A.4.

**Data Filtering and Refinement** To ensure the quality and validity of the collected data instances, we conduct manual filtering to exclude instances where the prompt fails to yield a renderable image or the associated visual elements are not uniquely identifiable. This filtering step reduced the initial 3,200 prompts to approximately 800 high-quality instances[2]. To expand the dataset while preserving both diversity and quality, we treat these 800 instances as seed T2I prompts, and design an iterative refinement process where GPT-4o is employed to generate additional T2I prompts and human experts are involved to evaluate them and provide targeted feedback to guide revisions, ensuring that each prompt adheres to the two guidelines. This iterative augmentation, as illustrated in Appendix A.3, continues until each reasoning subcategory reaches approximately 100 validated instances.

**Evaluation Criteria Generation and `R2I-Score`** Existing T2I evaluation metrics often fail to adequately assess the reasoning abilities essential for high-quality image generation. Hence, we create an evaluation set (i.e., a set of evaluation questions and their corresponding scoring criteria) tailored to each data instance in `R2I-Bench`. The carefully designed evaluation questions assess the T2I models in three core dimensions: ① *Text-image alignment*: whether the generated image accurately contains all required elements, such as objects and attributes; ② *Reasoning accuracy*: whether the T2I model performs necessary reasoning over the input prompt to correctly generate the output image; ③ *Image*

---

[2]Appendix A.3 provides detailed categories of filtered prompts.

*quality*: measuring the clarity and quality (e.g., vagueness, distortions, and so on) of the generated images. Example questions for each evaluation dimension are provided in Figure 2.

For efficiency, we feed each previously generated T2I prompt, the corresponding reference caption, and explanation description to GPT-4o and ask it to generate a set of evaluation questions, each paired with an assigned evaluation dimension, an importance weight, and a scoring criterion. Our preliminary study shows that, without constraints, GPT-4o consistently overemphasizes text–image alignment questions that are not directly related to reasoning. To better prioritize reasoning, we manually set a weight constraint range for each question based on its evaluation dimension: $[7, 10]$ for *reasoning accuracy*, $[4, 6]$ for *text-image alignment*, and $[1, 3]$ for *image quality*. The final weight for each evaluation question was determined by prompting GPT-4o to jointly consider all questions in context. This design reflects our goal of benchmarking reasoning-driven T2I generation, under the assumption that most modern T2I models already perform well in producing visually appealing images. To ensure reliability and consistency, all evaluation questions, scoring criteria, and importance weights are manually validated and refined by expert annotators. The complete instruction template in this process are provided in Appendix A.4.

Building on the evaluation set, we propose a new QA-style metric, `R2I-Score`. Given a generated image for a T2I prompt, we feed the image along with each evaluation question and its corresponding scoring criteria as input to GPT-4o, and ask it to select a score $s_i$ based on the provided criteria. This scoring instruction template is detailed in Ap-

pendix A.4. We calculate `R2I-Score` as follows:

$$\text{R2I-Score} = \frac{\sum_{i=1}^{n} w_i \cdot s_i}{\sum_{i=1}^{n} w_i} \qquad (1)$$

where $n$ is the total number of evaluation questions for a given instance, and $w_i$ is the importance weight assigned to the $i$-th evaluation question.

**Dataset Statistics** Finally, `R2I-Bench` comprises $3,068$ high-quality, reason-driven T2I prompts. Figure 1 includes an example T2I prompt for each core reasoning category, and Table 2 provides detailed statistics for `R2I-Bench`.

| Statistic | Number |
|---|---|
| Total data instances | 3,068 |
| - Commonsense | 695 (22.65%) |
| - Compositional | 311 (10.14%) |
| - Numerical | 322 (10.50%) |
| - Causal | 151 (4.92%) |
| - Mathematical | 800 (26.08%) |
| - Logical | 630 (20.53%) |
| - Concept Mixing | 159 (5.18%) |
| Categories | 7 |
| Subcategories | 32 |
| Evaluation dimensions | 3 |
| Vocabulary size | 7,184 |
| Maximum prompt length | 35 |
| Maximum reference caption length | 28 |
| Maximum evaluation questions | 18 |
| Average prompt length | 21.7 |
| Average reference caption length | 23.4 |
| Average evaluation questions | 12.2 |

Table 2: **Key Statistics of `R2I-Bench`.**

## 4 Experiments

### 4.1 Experimental Setup

To conduct evaluation on `R2I-Bench`, we carefully select 17 representative, high-performing T2I models with publicly available model checkpoints, spanning four distinct categories: (1) *Diffusion Models*, featuring models including `SD3-medium` (Rombach et al., 2022), `Lumina-Image 2.0` (Qin et al., 2025), `Sana-1.5` (Xie et al., 2025a), `Lumina-T2I` (Qin et al., 2025), `Omnigen` (Xiao et al., 2024), `LLM4GEN`$_{SD1.5}$ (Liu et al., 2025), and `ELLA`$_{SD1.5}$ (Hu et al., 2024); (2) *Autoregressive Models*, including `EMU3` (Wang et al., 2024), `Janus-Pro-7B` (Chen et al., 2025), `LlamaGen` (Sun et al., 2024a), and

`Show-o` (Xie et al., 2025b); (3) *Reasoning-Enhanced Models*, including `Show-o+ORM`, `Show-o+DPO`, and `Show-o+PARM` (Zhang et al., 2025) ; and (4) *Closed-Source Models*, including `DALL-E-3` (OpenAI, 2023) and `GPT-Image-1` (Hurst et al., 2024).

Additional implementation details, such as model architectures, configurations, and inference parameters, are provided in Appendix B. For evaluation, we adopt the proposed `R2I-Score` metric.

Intuitively, reasoning-driven T2I generation could be more effectively addressed by decoupling reasoning from image generation—first leveraging a large language model to perform complex reasoning and generate a detailed textual description, and then using a powerful image generation model to render the final image (Niu et al., 2025). Motivated by this, we design a strong pipeline-based framework that explicitly separates the reasoning and generation stages. The framework first employs a state-of-the-art LLM (`GPT-4o`) to interpret and reason over the original prompt, producing a detailed and structured image description. This rewritten prompt is then passed to a high-performing T2I model (`SD3-medium`) to generate the corresponding image. We name this pipelined framework as `gpt-4o+SD3-medium`.

### 4.2 Main Results

Table 3 presents the evaluation results of all T2I models across the core reasoning categories in `R2I-Bench`, with detailed subcategory-level results provided in Appendix B.1. The main findings are summarized as follows.

**T2I Models Show Limited Capability in Reasoning-Driven Image Generation.** Our evaluation reveals that most open-source models achieve a score lower than 45% based on `R2I-Score`, suggesting a notable gap in their ability to handle reasoning-driven T2I prompts. This limitation appears to stem from a shallow understanding of prompts, often interpreted as a bag of words rather than through compositional or logical reasoning. This hypothesis is further supported by our qualitative error analysis, illustrated in Appendix B.3, Figures 12 through 17, where the majority of models simply generate images that merely reflect the objects explicitly mentioned in the prompt without performing necessary inferential reasoning. For instance, given the prompt "*a cat-like bed*" (Figure 15), most of the mod-

| Model | Size | Overall | Commonsense | Compositional | Con.Mix | Logical | Numerical | Mathematical | Causal |
|---|---|---|---|---|---|---|---|---|---|
| *Diffusion Models* | | | | | | | | | |
| SD3-medium | 2B | 0.45 | 0.54 | 0.64 | 0.63 | 0.55 | 0.50 | 0.19 | 0.18 |
| Lumina-Image 2.0 | 2.6B | 0.42 | 0.49 | 0.65 | 0.54 | 0.56 | 0.43 | 0.13 | 0.40 |
| Sana-1.5 | 4.8B | 0.41 | 0.49 | 0.67 | 0.66 | 0.49 | 0.48 | 0.13 | 0.21 |
| Lumina-T2I | 5B | 0.33 | 0.38 | 0.49 | 0.55 | 0.38 | 0.45 | 0.13 | 0.18 |
| Omnigen | 3.8B | 0.40 | 0.43 | 0.60 | 0.43 | 0.51 | 0.47 | 0.18 | 0.34 |
| LLM4GEN$_{SD1.5}$ | 0.86B | 0.40 | 0.55 | 0.48 | 0.60 | 0.55 | 0.39 | 0.07 | 0.45 |
| ELLA$_{SD1.5}$ | 0.07B | 0.31 | 0.40 | 0.44 | 0.40 | 0.40 | 0.32 | 0.07 | 0.29 |
| *AutoRegressive Models* | | | | | | | | | |
| EMU3 | 8.0B | 0.41 | 0.44 | 0.59 | 0.62 | 0.55 | 0.61 | 0.09 | 0.41 |
| Janus-Pro-7B | 7B | 0.38 | 0.45 | 0.60 | 0.64 | 0.46 | 0.46 | 0.07 | 0.36 |
| LlamaGen | 0.8B | 0.29 | 0.38 | 0.39 | 0.49 | 0.38 | 0.35 | 0.07 | 0.12 |
| Show-o | 1.3B | 0.36 | 0.42 | 0.59 | 0.56 | 0.42 | 0.57 | 0.12 | 0.30 |
| *Reasoning-Enhanced Models* | | | | | | | | | |
| Show-o+ORM | 1.3B | 0.34 | 0.42 | 0.45 | 0.44 | 0.37 | 0.49 | 0.12 | 0.26 |
| Show-o+DPO | 1.3B | 0.36 | 0.43 | 0.47 | 0.48 | 0.41 | 0.51 | 0.13 | 0.31 |
| Show-o+PARM | 1.3B | 0.38 | 0.45 | 0.49 | 0.51 | 0.45 | 0.56 | 0.13 | 0.32 |
| *Close Source Models* | | | | | | | | | |
| DALL-E-3 | - | 0.71 | 0.78 | 0.76 | 0.86 | 0.69 | 0.69 | 0.21 | 0.64 |
| GPT-Image-1 | - | 0.77 | 0.83 | 0.87 | 0.89 | 0.81 | 0.88 | 0.58 | 0.71 |
| *Prompt-Rewrite Pipeline* | | | | | | | | | |
| gpt-4o+SD3-medium | 2B | 0.58$_{\uparrow 0.13}$ | 0.75$_{\uparrow 0.21}$ | 0.75$_{\uparrow 0.11}$ | 0.81$_{\uparrow 0.18}$ | 0.65$_{\uparrow 0.10}$ | 0.63$_{\uparrow 0.13}$ | 0.22$_{\uparrow 0.03}$ | 0.76$_{\uparrow 0.58}$ |

Table 3: **Evaluation on** `R2I-Bench`. The highest accuracy for closed-source and open-source text-to-image models are marked in red and blue respectively. The accuracy score is the average `R2I-Score` per model, and the overall score is computed as a micro average weighted by the number of instances in each category. Con.Mix.: Concept Mixing.

els, including `EMU3`, `SD3-medium`, `ELLA`, and `PARM+Show-o`, just naively depict a cat and a bed as distinct, unrelated objects. Similarly, in tasks involving logical operations or quantifiers such as the prompt "*either a spoon or a bowl*" (Figure 13), most models incorrectly render both objects, reflecting an inability to correctly interpret disjunctive semantics. We hypothesize that these limitations are rooted in the bag-of-words encoding mechanism used by CLIP-based conditioning in diffusion models. A formal investigation of this hypothesis is left for future work.

**Mathematical Reasoning Remains a Significant Bottleneck.** Across all reasoning categories, T2I models exhibit profound limitations in addressing mathematical reasoning tasks. Most models achieve near-zero accuracy on this front. Notably, even the best-performing open-source model, `SD3-medium`, attains a score of merely 0.19, while others, including `LlamaGen`, `Show-o`, and `ELLA`$_{SD1.5}$, score below 0.10. As shown in Figure 14, prompts involving geometric transformations (e.g., "*rotate a square 90°*") frequently result in irrelevant outputs such as abstract art or

clocks. Similarly, prompts grounded in number theory (e.g., "*visualize the twin prime pairs below 50*") yield outputs like mecha robots (`EMU3`) or glowing, non-descriptive artifacts (`Show-o+PARM`, `Show-o`). These observations indicate a severe lack of training data containing mathematical visual concepts, hindering the models' ability to perform reliable numerical or mathematical reasoning.

**Marginal Improvements from Reasoning-Enhanced Architectures.** Reasoning-enhanced models such as `Show-o+PARM`, `Show-o+ORM`, and `Show-o+DPO` demonstrate only incremental improvements over their respective base models. For example, the best-performing variant (i.e., `Show-o+PARM`) achieves an overall score of 0.38, compared to 0.36 achieved by the base model `Show-o`. Notably, these models continue to perform poorly on the most challenging categories, including mathematical reasoning ($\leq 0.13$) and causal reasoning ($\leq 0.32$), indicating that current methods, such as PARM (Potential Assessment Reward Model)(Lightman et al., 2024), ORM (Outcome Reward Model)(Cobbe et al., 2021), and DPO (Direct Preference Optimization)(Rafailov
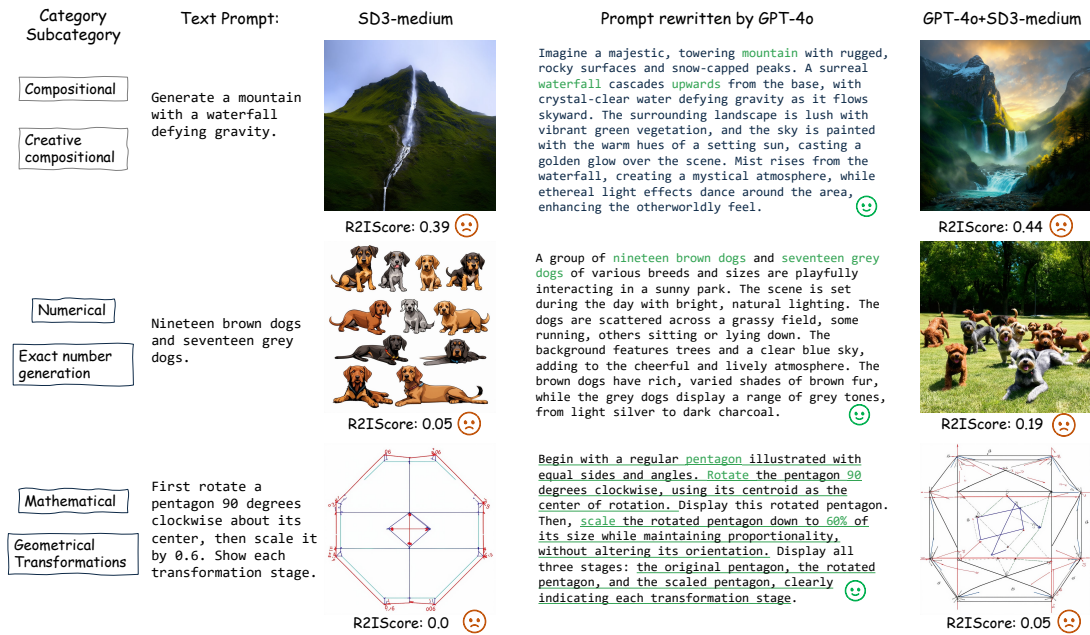
Figure 5: Failure Cases of the Pipeline-based Framework on Compositional/Numerical/Mathematical Reasoning.

et al., 2023), offer limited improvements in reasoning-driven T2I generation. These results highlight the urgent need for more effective and targeted approaches for reasoning-driven T2I generation.

**Closed-Source Models Set the Upper Bound for Current Reasoning Capabilities.** Proprietary models such as DALLE-3 and GPT-Image-1 substantially outperform their open-source counterparts, surpassing the best-performing open-source model (i.e., SD3-medium) by 57.8% and 71.1%, respectively. In particular, GPT-Image-1 consistently achieves the highest scores across all reasoning categories. More recently, Nano-Banana (Team, 2025) reported the state-of-the-art performance in image generation and editing. We further provide comprehensive quantitative and qualitative analyses of Nano-Banana in Appendix B.6, where we find that its performance is notably less competitive than that of DALLE-3 or GPT-Image-1. The suboptimal performance of proprietary models highlights the pressing need for open, reproducible benchmarks and the development of competitive open-source T2I models to bridge the capability gap with proprietary systems.

**Pipeline-based T2I Framework Improves Commonsense, Causal Reasoning, but Yields Marginal Gains for Compositional, Numerical and Mathematical Reasoning.** As shown in Table 3, the pipeline-based framework yields substantial gains in all reasoning categories by an average of 0.13, e.g., improvements ranging from 0.21 to 0.58 are observed in causal reasoning, commonsense reasoning. A detailed comparison across fine-grained reasoning subcategories is shown in Figure 10 in Appendix B.4. Despite the general effectiveness of the pipeline-based framework, gains in *Compositional*, *Mathematical* categories remain modest ($\leq 0.13$). As shown in Figure 5, many reasoning concepts remain challenging for T2I models to faithfully render, even when clearly articulated by the LLM. In *Compositional reasoning* (Example 1), despite GPT-4o correctly reasons that "*a surreal waterfall cascades upwards from the base*," SD3-medium still renders a downward-flowing waterfall. In *Numerical reasoning* (Example 2), although GPT-4o expands the original prompt "*Nineteen brown dogs and seventeen grey dogs*" with additional details, the generated image fails to depict the correct number of dogs. For *Mathematical reasoning* (Example 3), the difficulty goes beyond language to abstract cognition: although GPT-4o specifies terms like "*display all three stages*" and "*regular pentagon*," the output remains visually inaccurate, with SD3-medium producing disorganized geometric shapes. Success in this domain often requires models to grasp geometric structures such as points, lines, angles, and spatial transformations. We posit that overcoming these limitations will require not only more

mathematically enriched training data but also the integration of architectural components or external modules capable of reasoning over structured symbolic knowledge.

### 4.3 Evaluation of `R2I-Score`

We further assess the effectiveness of our proposed `R2I-Score` by evaluating its alignment with human judgments. We conduct a human study involving a group of senior college students, where each participant compares the image outputs generated by two T2I models, `Lumina-Image 2.0` (Qin et al., 2025) and `Sana-1.5` (Xie et al., 2025a), and selects the image that best aligns with the prompts or indicates if both are equally satisfactory or unsatisfactory. More details are provided in Appendix B.2. We also apply `R2I-Score` to evaluate the same set of image pairs and compare its judgements with those of human annotators, using three established evaluation metrics: *Pairwise Accuracy* (Deutsch et al., 2023), *Kendall's $\tau$* (Jadhav and Ma, 2019), and *Spearman Correlation* (Tu et al., 2025). We compare `R2I-Score` against several widely adopted T2I generation evaluation metrics, including **DSGscore** (Cho et al., 2024), **VIEScore** (Ku et al., 2024), **CLIPScore** (Hessel et al., 2021), and **VQA score** (Lin et al., 2024). Since these existing metrics mainly focus on surface-level text-image alignment and image quality, `R2I-Score` consistently achieves superior alignment with human judgements across all metrics, as shown in Table 4, demonstrating its effectiveness and robustness as an evaluation metric of reasoning-driven T2I generation. Further experimental details and additional results are provided in Appendix B.5.

| Models | Pairwise Accuracy | Kendall's $\tau$ | Spearman Correlation |
|---|---|---|---|
| CLIPScore | 0.631 | 0.263 | 0.310 |
| DSGScore | 0.520 | 0.220 | 0.254 |
| VIEScore | 0.694 | 0.494 | 0.451 |
| VQAscore | 0.629 | 0.463 | 0.563 |
| R2I-Score | **0.713** | **0.747** | **0.694** |

Table 4: Comparison of `R2I-Score` with other Evaluation Metrics for T2I Generation.

### 4.4 Error Analysis

To better understand the limitations of current T2I models, we categorize their failure cases based on the three evaluation dimensions used in `R2I-Score`, and accordingly define three failure types: *basic element errors*, *reasoning errors*, and

*visual quality issues*. For qualitative analysis, we examine representative models from each architectural category, including `Emu3`, `SD3-medium`, `Show-o+PARM`, and `GPT-Image-1`. The relative distribution of these failure types is computed and visualized in Figure 6. As we can see, reasoning-related failures dominate the error distribution across all four models, accounting for over 80% of total errors. This observation highlights reasoning as the primary bottleneck in current T2I systems. Among the evaluated models, `Show-o+PARM` exhibits a relatively higher proportion of basic element errors, suggesting its limitation in accurately rendering basic visual components. In contrast, `GPT-Image-1` demonstrates the lowest rates of both basic element and image quality errors, indicating its superior performance in both semantic fidelity and visual rendering.
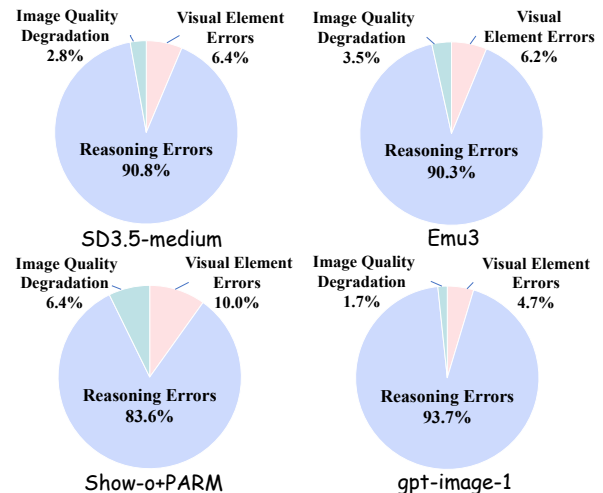


Figure 6: Distribution of Errors of `Emu3`, `SD3-medium`, `Show-o+PARM`, `GPT-Image-1`.

## 5 Conclusion

This paper introduces `R2I-Bench`, a comprehensive benchmark designed to evaluate the reasoning capabilities of text-to-image (T2I) generation models across 7 core reasoning categories and 32 subcategories. Alongside `R2I-Bench`, we design `R2I-Score`, a QA-style evaluation metric specifically tailored for reasoning-driven T2I generation, with stronger correlation with human judgments compared to existing evaluation metrics. Our evaluation reveals consistently limited reasoning capabilities across all existing T2I models, highlighting the pressing need for more robust, reasoning-aware T2I generation architectures.

## Limitations

**Evaluation Method Constraints** Despite our diligent efforts to design and refine evaluation questions and criteria for each data instance, aimed at enhancing reasoning-based evaluation, the current method is inherently constrained by the specific benchmark used in this study. As such, it cannot be directly generalized to other datasets without further adaptations. Although the manually crafted evaluation questions and criteria facilitate the use of vision language models for scoring, leading to more transparent and interpretable evaluations, the granularity of these evaluations remains relatively coarse compared to the detailed assessments conducted at the training level. Future work could focus on the development of a versatile reward model tailored for evaluating Text-to-Image (T2I) reasoning generation, which would also support reinforcement learning from Human Feedback (RLHF).

**Language and Dataset Scope** At present, our evaluation of T2I models is confined to `R2I-Bench`, which is based solely on English-language data. Consequently, the reasoning capabilities of models in non-English language contexts remain unexplored. Additionally, some models do not support symbolic inputs, such as emojis or complex mathematical notations. For the sake of ensuring the benchmark's general applicability, we have excluded data instances that feature such symbolic inputs. Besides, our benchmark is limited only to image generation. Extending to video/audio/3D generation can be another promising future direction.

## Ethics Statement

Some instances in our dataset were generated using `GPT-4o`, a powerful language model that has been designed to simulate human-like text generation. Although this model produces high-quality outputs, it is important to note that the generated content reflects the biases and limitations inherent in the training data. We are aware of the ethical implications of using such models, especially in terms of the potential for reinforcing harmful stereotypes or generating inappropriate content. In this study, we have made efforts to mitigate these risks by carefully curating the dataset and implementing a manual review process. However, we acknowledge that there may still be residual biases present, and we encourage future work to focus on developing methods to reduce such biases, ensuring that generated content aligns with ethical guidelines and societal norms.

## Acknowledgement

## References

Nitzan Bitton-Guetta, Aviv Slobodkin, Aviya Maimon, Eliya Habba, Royi Rassin, Yonatan Bitton, Idan Szpektor, Amir Globerson, and Yuval Elovici. 2024. Visual riddles: a commonsense and world knowledge challenge for large vision and language models. *Advances in Neural Information Processing Systems*, 37:139561–139588.

Liang Chen, Sinan Tan, Zefan Cai, Weichu Xie, Haozhe Zhao, Yichi Zhang, Junyang Lin, Jinze Bai, Tianyu Liu, and Baobao Chang. 2024. A spark of vision-language intelligence: 2-dimensional autoregressive transformer for efficient finegrained image generation. In *Proceedings of the 13th International Conference on Learning Representations (ICLR)*.

Xiaokang Chen, Zhiyu Wu, Xingchao Liu, Zizheng Pan, Wen Liu, Zhenda Xie, Xingkai Yu, and Chong Ruan. 2025. Janus-pro: Unified multimodal understanding and generation with data and model scaling. *arXiv preprint arXiv:2501.17811*.

Mathieu Chevalley, Yusuf Roohani, Arash Mehrjou, Jure Leskovec, and Patrick Schwab. 2022. Causalbench: A large-scale benchmark for network inference from single-cell perturbation data. *arXiv preprint arXiv:2210.17283*.

Jaemin Cho, Yushi Hu, Roopal Garg, Peter Anderson, Ranjay Krishna, Jason Baldridge, Mohit Bansal, Jordi Pont-Tuset, and Su Wang. 2024. Davidsonian scene graph: Improving reliability in fine-grained evaluation for text-to-image generation. In *Proceedings of the Twelfth International Conference on Learning Representations (ICLR)*.

Karl Cobbe, Vineet Kosaraju, Mohammad Bavarian, Mark Chen, Heewoo Jun, Lukasz Kaiser, Matthias Plappert, Jerry Tworek, Jacob Hilton, Reiichiro

Nakano, et al. 2021. Training verifiers to solve math word problems. *arXiv preprint arXiv:2110.14168*.

Daniel Deutsch, George Foster, and Markus Freitag. 2023. Ties matter: Meta-evaluating modern metrics with pairwise accuracy and tie calibration. In *Proceedings of the 2023 Conference on Empirical Methods in Natural Language Processing (EMNLP)*.

Patrick Esser, Sumith Kulal, Andreas Blattmann, Rahim Entezari, Jonas Müller, Harry Saini, Yam Levi, Dominik Lorenz, Axel Sauer, Frederic Boesel, Dustin Podell, Tim Dockhorn, Zion English, and Robin Rombach. 2024. Scaling rectified flow transformers for high-resolution image synthesis. In *Proceedings of the 41st International Conference on Machine Learning (ICML)*.

Xingyu Fu, Muyu He, Yujie Lu, William Yang Wang, and Dan Roth. 2024. Commonsense-t2i challenge: Can text-to-image generation models understand commonsense? In *Proceedings of the First Conference on Language Modeling (COLM)*.

Peng Gao, Le Zhuo, Dongyang Liu, Ruoyi Du, Xu Luo, Longtian Qiu, Yuhang Zhang, Rongjie Huang, Shijie Geng, Renrui Zhang, Junlin Xie, Wenqi Shao, Zhengkai Jiang, Tianshuo Yang, Weicai Ye, Tong He, Jingwen He, Junjun He, Yu Qiao, and Hongsheng Li. 2025. Lumina-t2x: Scalable flow-based large diffusion transformer for flexible resolution generation. In *Proceedings of the 13th International Conference on Learning Representations (ICLR)*.

Dhruba Ghosh, Hannaneh Hajishirzi, and Ludwig Schmidt. 2023. Geneval: An object-focused framework for evaluating text-to-image alignment. *Advances in Neural Information Processing Systems*, 36:52132–52152.

Jack Hessel, Ari Holtzman, Maxwell Forbes, Ronan Le Bras, and Yejin Choi. 2021. Clipscore: A reference-free evaluation metric for image captioning. In *Proceedings of the 2021 Conference on Empirical Methods in Natural Language Processing*, pages 7514–7528. Association for Computational Linguistics.

Xiwei Hu, Rui Wang, Yixiao Fang, Bin Fu, Pei Cheng, and Gang Yu. 2024. Ella: Equip diffusion models with llm for enhanced semantic alignment. *arXiv preprint arXiv:2403.05135*.

Aaron Hurst, Adam Lerer, Adam P Goucher, Adam Perelman, Aditya Ramesh, Aidan Clark, AJ Ostrow, Akila Welihinda, Alan Hayes, Alec Radford, et al. 2024. Gpt-4o system card. *arXiv preprint arXiv:2410.21276*.

Sneha Jadhav and Shuangge Ma. 2019. Kendall's tau for functional data analysis. *arXiv preprint arXiv:1912.03725*.

Dongzhi Jiang, Ziyu Guo, Renrui Zhang, Zhuofan Zong, Hao Li, Le Zhuo, Shilin Yan, Pheng-Ann Heng, and Hongsheng Li. 2025. T2i-r1: Reinforcing image generation with collaborative semantic-level and token-level cot. *arXiv preprint arXiv:2505.00703*.

Ivana Kajić, Olivia Wiles, Isabela Albuquerque, Matthias Bauer, Su Wang, Jordi Pont-Tuset, and Aida Nematzadeh. 2024. Evaluating numerical reasoning in text-to-image models. *Advances in Neural Information Processing Systems*, 37:42211–42224.

Max Ku, Dongfu Jiang, Cong Wei, Xiang Yue, and Wenhu Chen. 2024. VIEScore: Towards explainable metrics for conditional image synthesis evaluation. In *Proceedings of the 62nd Annual Meeting of the Association for Computational Linguistics (Volume 1: Long Papers)*, pages 12268–12290. Association for Computational Linguistics.

Tony Lee, Michihiro Yasunaga, Chenlin Meng, Yifan Mai, Joon Sung Park, Agrim Gupta, Yunzhi Zhang, Deepak Narayanan, Hannah Teufel, Marco Bellagente, et al. 2023. Holistic evaluation of text-to-image models. *Advances in Neural Information Processing Systems*, 36:69981–70011.

Baiqi Li, Zhiqiu Lin, Deepak Pathak, Jiayao Emily Li, Xide Xia, Graham Neubig, Pengchuan Zhang, and Deva Ramanan. 2024. GenAI-bench: A holistic benchmark for compositional text-to-visual generation. In *Proceedings of the IEEE/CVF Conference on Computer Vision and Pattern Recognition (CVPR) Workshops*.

Jiaqi Liao, Zhengyuan Yang, Linjie Li, Dianqi Li, Kevin Lin, Yu Cheng, and Lijuan Wang. 2025. Imagegen-cot: Enhancing text-to-image in-context learning with chain-of-thought reasoning. *arXiv preprint arXiv:2503.19312*.

Jun Hao Liew, Hanshu Yan, Daquan Zhou, and Jiashi Feng. 2022. Magicmix: Semantic mixing with diffusion models. *arXiv preprint arXiv:2210.16056*.

Hunter Lightman, Vineet Kosaraju, Yuri Burda, Harrison Edwards, Bowen Baker, Teddy Lee, Jan Leike, John Schulman, Ilya Sutskever, and Karl Cobbe. 2024. Let's verify step by step. In *Proceedings of the 12th International Conference on Learning Representations (ICLR)*.

Zhiqiu Lin, Deepak Pathak, Baiqi Li, Jiayao Li, Xide Xia, Graham Neubig, Pengchuan Zhang, and Deva Ramanan. 2024. Evaluating text-to-visual generation with image-to-text generation. In *Proceedings of the European Conference on Computer Vision (ECCV)*, pages 366–384. Springer.

Jian Liu, Leyang Cui, Hanmeng Liu, Dandan Huang, Yile Wang, and Yue Zhang. 2020. Logiqa: A challenge dataset for machine reading comprehension with logical reasoning. In *Proceedings of the Twenty-Ninth International Joint Conference on Artificial Intelligence*, pages 3622–3628. International Joint Conferences on Artificial Intelligence Organization.

Mushui Liu, Yuhang Ma, Zhen Yang, Jun Dan, Yunlong Yu, Zeng Zhao, Zhipeng Hu, Bai Liu, and Changjie Fan. 2025. Llm4gen: Leveraging semantic representation of llms for text-to-image generation. In *Proceedings of the Thirty-Ninth AAAI Conference on*

*Artificial Intelligence (AAAI-25)*, volume 39, pages 5523–5531.

Yujie Lu, Xianjun Yang, Xiujun Li, Xin Eric Wang, and William Yang Wang. 2023. Llmscore: Unveiling the power of large language models in text-to-image synthesis evaluation. *Advances in Neural Information Processing Systems*, 36:23075–23093.

Kenneth Marino, Mohammad Rastegari, Ali Farhadi, and Roozbeh Mottaghi. 2019. Ok-vqa: A visual question answering benchmark requiring external knowledge. In *Proceedings of the IEEE/CVF Conference on Computer Vision and Pattern Recognition (CVPR)*, pages 3195–3204.

Yuwei Niu, Munan Ning, Mengren Zheng, Bin Lin, Peng Jin, Jiaqi Liao, Kunpeng Ning, Bin Zhu, and Li Yuan. 2025. Wise: A world knowledge-informed semantic evaluation for text-to-image generation. *arXiv preprint arXiv:2503.07265*.

OpenAI. 2023. Dall·e 3. `https://openai.com/dall-e-3/`. Accessed: 2025-09-12.

Jingyuan Qi, Zhiyang Xu, Qifan Wang, and Lifu Huang. 2025. Ar-rag: Autoregressive retrieval augmentation for image generation. *arXiv preprint arXiv:2506.06962*.

Qi Qin, Le Zhuo, Yi Xin, Ruoyi Du, Zhen Li, Bin Fu, Yiting Lu, Jiakang Yuan, Xinyue Li, Dongyang Liu, et al. 2025. Lumina-image 2.0: A unified and efficient image generative framework. *arXiv preprint arXiv:2503.21758*.

Rafael Rafailov, Archit Sharma, Eric Mitchell, Christopher D Manning, Stefano Ermon, and Chelsea Finn. 2023. Direct preference optimization: Your language model is secretly a reward model. In *Advances in Neural Information Processing Systems (NeurIPS)*.

Robin Rombach, Andreas Blattmann, Dominik Lorenz, Patrick Esser, and Bjorn Ommer. 2022. High-resolution image synthesis with latent diffusion models. In *Proceedings of the IEEE/CVF Conference on Computer Vision and Pattern Recognition (CVPR)*, pages 10684–10695.

Ying Shen, Zhiyang Xu, Jiuhai Chen, Shizhe Diao, Jiaxin Zhang, Yuguang Yao, Joy Rimchala, Ismini Lourentzou, and Lifu Huang. 2025. Latte-flow: Layerwise timestep-expert flow-based transformer. *arXiv preprint arXiv:2506.06952*.

Peize Sun, Yi Jiang, Shoufa Chen, Shilong Zhang, Bingyue Peng, Ping Luo, and Zehuan Yuan. 2024a. Autoregressive model beats diffusion: Llama for scalable image generation. *arXiv preprint arXiv:2406.06525*.

Quan Sun, Yufeng Cui, Xiaosong Zhang, Fan Zhang, Qiying Yu, Yueze Wang, Yongming Rao, Jingjing Liu, Tiejun Huang, and Xinlong Wang. 2024b. Generative multimodal models are in-context learners. In

*Proceedings of the IEEE/CVF Conference on Computer Vision and Pattern Recognition (CVPR)*, pages 14398–14409.

Quan Sun, Qiying Yu, Yufeng Cui, Fan Zhang, Xiaosong Zhang, Yueze Wang, Hongcheng Gao, Jingjing Liu, Tiejun Huang, and Xinlong Wang. 2023. Emu: Generative pretraining in multimodality. *arXiv preprint arXiv:2307.05222*.

Gemini Team. 2025. Gemini 2.5: Pushing the frontier with advanced reasoning, multimodality, long context, and next generation agentic capabilities.

Tristan Thrush, Ryan Jiang, Max Bartolo, Amanpreet Singh, Adina Williams, Douwe Kiela, and Candace Ross. 2022. Winoground: Probing vision and language models for visio-linguistic compositionality. In *Proceedings of the IEEE/CVF Conference on Computer Vision and Pattern Recognition (CVPR)*, pages 5238–5248.

Shengbang Tong, David Fan, Jiachen Zhu, Yunyang Xiong, Xinlei Chen, Koustuv Sinha, Michael Rabbat, Yann LeCun, Saining Xie, and Zhuang Liu. 2024. Metamorph: Multimodal understanding and generation via instruction tuning. *arXiv preprint arXiv:2412.14164*.

Shengxin Tu, Chun Li, and Bryan E Shepherd. 2025. Between-and within-cluster spearman rank correlations. *Statistics in Medicine*, 44(3-4):e10326.

Xinlong Wang, Xiaosong Zhang, Zhengxiong Luo, Quan Sun, Yufeng Cui, Jinsheng Wang, Fan Zhang, Yueze Wang, Zhen Li, Qiying Yu, et al. 2024. Emu3: Next-token prediction is all you need. *arXiv preprint arXiv:2409.18869*.

Xindi Wu, Dingli Yu, Yangsibo Huang, Olga Russakovsky, and Sanjeev Arora. 2024. Conceptmix: A compositional image generation benchmark with controllable difficulty. In *Advances in Neural Information Processing Systems (NeurIPS), Datasets and Benchmarks Track*.

Shitao Xiao, Yueze Wang, Junjie Zhou, Huaying Yuan, Xingrun Xing, Ruiran Yan, Chaofan Li, Shuting Wang, Tiejun Huang, and Zheng Liu. 2024. Omnigen: Unified image generation. *arXiv preprint arXiv:2409.11340*.

Enze Xie, Junsong Chen, Yuyang Zhao, Jincheng Yu, Ligeng Zhu, Chengyue Wu, Yujun Lin, Zhekai Zhang, Muyang Li, Junyu Chen, et al. 2025a. Sana 1.5: Efficient scaling of training-time and inference-time compute in linear diffusion transformer. *arXiv preprint arXiv:2501.18427*.

Jinheng Xie, Weijia Mao, Zechen Bai, David Junhao Zhang, Weihao Wang, Kevin Qinghong Lin, Yuchao Gu, Zhijie Chen, Zhenheng Yang, and Mike Zheng Shou. 2025b. Show-o: One single transformer to unify multimodal understanding and generation. In *Proceedings of the 13th International Conference on Learning Representations (ICLR)*.

Zhiyang Xu, Jiuhai Chen, Zhaojiang Lin, Xichen Pan, Lifu Huang, Tianyi Zhou, Madian Khabsa, Qifan Wang, Di Jin, Michihiro Yasunaga, et al. 2025. Pisces: An auto-regressive foundation model for image understanding and generation. *arXiv preprint arXiv:2506.10395*.

Zhiyang Xu, Minqian Liu, Ying Shen, Joy Rimchala, Jiaxin Zhang, Qifan Wang, Yu Cheng, and Lifu Huang. Modality-specialized synergizers for interleaved vision-language generalists. In *The Thirteenth International Conference on Learning Representations*.

Ling Yang, Jingwei Liu, Shenda Hong, Zhilong Zhang, Zhilin Huang, Zheming Cai, Wentao Zhang, and Bin Cui. 2023. Improving diffusion-based image synthesis with context prediction. *Advances in Neural Information Processing Systems*, 36:37636–37656.

Qian Zhang, Xiangzi Dai, Ninghua Yang, Xiang An, Ziyong Feng, and Xingyu Ren. 2024. Var-clip: Text-to-image generator with visual auto-regressive modeling. *arXiv preprint arXiv:2408.01181*.

Renrui Zhang, Chengzhuo Tong, Zhizheng Zhao, Ziyu Guo, Haoquan Zhang, Manyuan Zhang, Jiaming Liu, Peng Gao, and Hongsheng Li. 2025. Let's verify and reinforce image generation step by step. In *Proceedings of the IEEE/CVF Conference on Computer Vision and Pattern Recognition (CVPR)*, pages 28662–28672.

Xiangyu Zhao, Peiyuan Zhang, Kexian Tang, Hao Li, Zicheng Zhang, Guangtao Zhai, Junchi Yan, Hua Yang, Xue Yang, and Haodong Duan. 2025. Envisioning beyond the pixels: Benchmarking reasoning-informed visual editing. *arXiv preprint arXiv:2504.02826*.

Chunting Zhou, LILI YU, Arun Babu, Kushal Tirumala, Michihiro Yasunaga, Leonid Shamis, Jacob Kahn, Xuezhe Ma, Luke Zettlemoyer, and Omer Levy. 2025. Transfusion: Predict the next token and diffuse images with one multi-modal model. In *Proceedings of the 13th International Conference on Learning Representations (ICLR)*.

Xiangru Zhu, Penglei Sun, Yaoxian Song, Yanghua Xiao, Zhixu Li, Chengyu Wang, Jun Huang, Bei Yang, and Xiaoxiao Xu. 2025. Evaluating semantic variation in text-to-image synthesis: A causal perspective. In *Proceedings of the 13th International Conference on Learning Representations (ICLR)*.

# A Dataset Construction Details

## A.1 Determination of the Number of Questions for Each Prompt

**Text-Image Alignment:** The number of questions is determined based on the objects, attributes, and relationships described in the prompt. For each element, a corresponding question is generated to assess the alignment between the text and the generated image.

**Reasoning Accuracy:** The number of questions in this category is based on the reasoning points identified in the prompt. For each reasoning step required (e.g., comparisons, causality), a question is created to evaluate the accuracy of the reasoning.

**Image Quality:** The number of questions related to image quality is determined by the reasoning points in the prompt. Each reasoning point generates a question to assess how well the image reflects the reasoning. This is particularly important because the model may generate unrealistic or distorted outputs when dealing with unfamiliar reasoning points. Additionally, an overall question is included to evaluate the general quality of the image.

## A.2 Definition of Categories in R2I-Bench

The data instances in R2I-Bench encompass seven core categories: Commonsense Reasoning, Compositional Reasoning, Conceptual Mixing Reasoning, Numerical Reasoning, Logical Reasoning, Causal Reasoning, and Mathematical Reasoning. These categories are further subdivided into thirty-two more granular subcategories, providing a thorough evaluation of the reasoning capabilities of Text-to-Image (T2I) models.

**Commonsense Reasoning** Commonsense reasoning is a critical aspect of evaluating a model's understanding of general knowledge and contextual information. It involves utilizing external *knowledge resources*—such as *world knowledge*, *cultural context*, or *background information*—to reason about the content of an image, rather than simply replicating the image. This allows for a richer context in assessing the commonsense reasoning capabilities of *Text-to-Image* (T2I) models. In R2I-Bench, we categorize commonsense reasoning into seven distinct *subfields*, as shown in Figure 12, with detailed definitions provided in Table 12.

**Compositional Reasoning** Compositional reasoning refers to the ability to combine smaller, simpler *components* or pieces of *information* to form more complex *concepts*, *solutions*, or *conclusions*. It involves understanding the *relationships* between individual parts and how they contribute to the whole, enabling *logical reasoning* within structured, hierarchical, or layered systems. In R2I-Bench, we divide compositional reasoning into three *subfields*, as depicted in Figure 16, with their definitions outlined in Table 9.

**Numerical Reasoning** Numerical reasoning, in the context of T2I models, involves the ability of these models to accurately interpret, process, and generate *images* based on *numerical information* presented in *textual prompts*. In R2I-Bench, we categorize numerical reasoning into three *subfields*, as illustrated in Figure 18, with definitions provided in Table 11.

**Concept Mixing Reasoning** Concept-Mixing reasoning refers to the process of combining different *semantic elements* to create a new, unique *concept*. In R2I-Bench, we divide concept-mixing reasoning into three *subfields*, as shown in Figure 15, with their definitions in Table 7.

**Logical Reasoning** Logical reasoning involves using systematic, structured approaches to analyze *information*, draw *conclusions*, and solve *problems* based on given *premises* or *conditions*. In R2I-Bench, we break logical reasoning down into seven *subfields*, as illustrated in Figure 13, with definitions provided in Table 10.

**Mathematical Reasoning** Mathematical reasoning refers to the ability to represent, understand, and generate visual representations of abstract *mathematical concepts* and *symbols*. In R2I-Bench, we subdivide mathematical reasoning into eight *subfields*, as shown in Figure 14, with their definitions outlined in Table 6.

**Causal Reasoning** Causal reasoning is the ability to understand and explain *cause-and-effect relationships*. In R2I-Bench, we categorize causal reasoning into three *subfields*, as illustrated in Figure 17, with definitions provided in Table 8.

**Definition of Subcategories in R2I-Bench** This section presents definitions of various subcategories under categories in R2I-Bench. Table 6 to 12 coresponding to subcategories under the categories of *Commonsense Reasoning, Numerical*

*Reasoning, Causal Reasoning, Logical Reasoning, Mathematical Reasoning, Concept Mixing Reasoning, Compositional Reasoning*, respectively.

**Clarifying Category Boundaries in `R2I-Bench`** numerical reasoning is focused on generating images based on *numerical information in textual prompts*, while mathematical reasoning is more about *visual representations of abstract mathematical concepts and symbols*. The weight of evaluation questions requiring accurate numerical rendering and spatial relations is relatively low, since numerical counting and spatial relations are not considered part of the core reasoning scope of mathematical reasoning. Spatial reasoning is specifically evaluated within the compositional reasoning category, while numerical and mathematical reasoning are assessed within their respective categories.
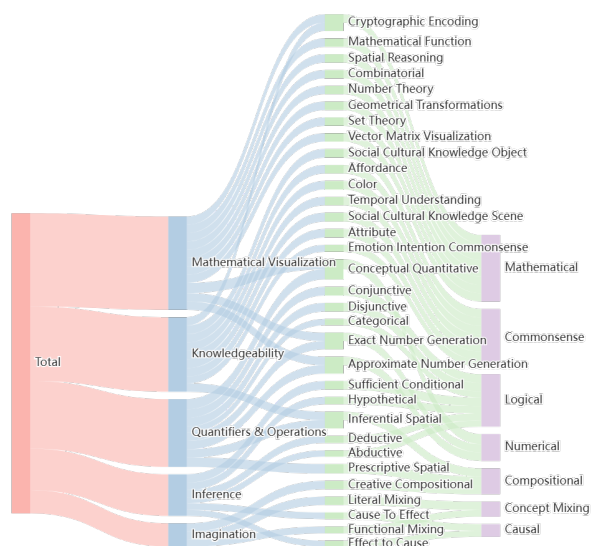


Figure 7: Distribution of reasoning abilities, subcategories, and categories in `R2I-Bench`.

**Negative Examples in Prompt Generation** We categorize negative examples into two main types:

(1) No Effective Reasoning. These are prompts that explicitly reveal the reasoning process, making the task trivial for the model. For example, in the commonsense reasoning subcategory *color*, the prompt

*A red apple on a white tablecloth.*

is a poor case because the color information is provided directly in the prompt, leaving no need for reasoning.

(2) Non-Unique Answer. These are prompts where the expected output (ground truth) is neither unique nor deterministic. For instance,

*Generate an image of a boy's reaction when he sees his exam score.*

is a negative example because the reaction is unconstrained: the boy could be happy, sad, or show any other emotion. Such vagueness prevents the prompt from yielding a unique and identifiable output.

### A.3 Prompt Filtering Process Details

The initial prompt pool contained approximately $3,200$ prompts. After several rounds of filtering and validation, we retained 800 high-quality prompts. The filtering was based on prompt quality, which included *non-unique answers*, *repetitive prompts*, and *lack of effective reasoning*. A detailed breakdown is as follows:

(1) No Effective Reasoning: Around 660 prompts were removed due to a lack of meaningful reasoning.

(2) Non-Unique Answer: About 690 prompts were discarded because they referred to multiple possible answers, making them ambiguous.

(3) Repetitive or Low-Linguistic-Diversity Prompts: Approximately $1,050$ prompts were removed for being repetitive or lacking variety in vocabulary.

**Iterative Prompt Refinement** To clarify the iterative process used to refine the final prompt set, we conducted three iterations in total. Each iteration involved both expansion and filtering to improve quality and diversity:

(1) First iteration: The prompt set was expanded from 800 to $3,200$ prompts, with approximately $2,400$ new prompts added.

(2) Second iteration: We removed duplicate prompts, non-unique answers, and prompts with ineffective reasoning, totaling approximately $1,200$ removals. At the same time, about $1,200$ new prompts were added, keeping the total at $3,200$.

(3) Third iteration: In the final round, around 232 unqualified prompts were removed, and approximately 100 new prompts were added, resulting in a final set of $3,068$ prompts.

**Annotation Quality Control** Three senior PhD students cross-checked and reviewed the data in `R2I-Bench`, offering feedback and validating the results. The multiple rounds of feedback and discussions among the annotators helped ensure consistency in the annotations.

Using the same model for prompt generation may result in repeated prompts and objects, thereby

Table 5: Human annotation details

| Metric | Value |
|---|---|
| Avg. Time per Instance | ~45–60 sec |
| Price per Instance | $0.04 USD |

limiting language diversity. To alleviate this issue, we adopted category-specific strategies. For example, in the case of numerical reasoning, we first instructed the model to generate a set of unique objects, such as office supplies or household items. These objects were subsequently incorporated into prompts such as *"There are more xxx than xxx "* and *"The number of xxx is as many as xxx."* Furthermore, we manually examined prompt diversity during the data filtering stage to ensure variation and reduce redundancy.

### A.4 Prompts details

During the prompt generation process, we observed that a substantial portion of the generated prompts were of low quality or duplicated. Directly generating explanation outputs, evaluation questions, and weights for these prompts would introduce unnecessary API costs without contributing to the quality of the benchmark. To address this issue and improve efficiency, we first filter out low-quality and duplicate prompts. Only after this filtering step do we proceed to generate explanation outputs, evaluation questions, and weights.

**Prompt for Data Instances Creation** We initially generate data instance using `gpt-4o` with the following prompt and deleted lots of duplicated and low-quality data instances in data filtering stage.

```
### Good Cases
[SUBCATEGORY GOOD CASES]

### Incorrect Implementation Example
Here are some WRONG IMPLEMENTATION you will make:

[SUBCATEGORY BAD CASES]
### Output Format:
```json
{
  "Prompt": "xxx",
  "Reference Caption": "xxx"
}
"""
```

**Prompt for Explanation Generation** We generate explanations using `GPT-4o` with the following prompt.

**Prompt for Explanation Generation**

```
EXPLANATION_GENERATION_PROMPT = """
Following is a prompt focused on testing the reasoning
↪  capabilities of a text-to-image generation model.
Prompt: [PROMPT]
Reference Caption: [REFERENCE CAPTION]
Your task is to explain why the correct answer
↪  corresponding to the Prompt is the Reference
↪  Caption.
### Output Format:
```json
{
  "Explanation": "xxx"
}
"""
```

**Prompt for Image Evaluation** After refining the evaluation questions and scoring criteria, we use these prompts with the state-of-the-art visual language model, GPT-4o, with a fixed temperature of 0.1, to obtain scores for each image relative to its corresponding text.

**Prompt for data instances creation**

```
DATA_CREATION_PROMPT="""
You are an expert in text-to-image generation. I am
↪  currently creating a benchmark to test the
↪  reasoning ability of text-to-image generation
↪  models.

### Definition of [CATEGORY]:
[CATEGORY DEFINITIN]

### Definition of [SUBCATEGORY]:
[SUBCATEGORY DEFINITIN]
### Task:
Can you generate 10 test cases for [SUBCATEGORY] to
↪  evaluate the text-to-image model's reasoning
↪  ability?

### Notices:
1. The prompt should not explicitly mention the
↪  aspects that require reasoning, in order to avoid
↪  leaking the reasoning process.
2. Ensure that your ground truth is **uniquely
↪  determinable**.
```

**Prompt for Image Evaluation**

```
IMAGE_EVALUATION_PROMPT = """
# Text-to-Image Quality Evaluation Protocol

## System Instructions
You are an AI quality auditor for text-to-image
↪  generation. Your task is to evaluate images with
↪  ABSOLUTE RUTHLESSNESS. Only images that meet the
↪  HIGHEST standards should receive the top scores.

## Task Overview
The image is generated based on the following prompt:
[PROMPT]

## Evaluation Criteria
[QUESTION LIST]

## Output Format
You may provide an analysis in your output, but ensure
↪  that the final line is formatted as shown below:

## Important Enforcement
[IMPORTANT ENFORCEMENT]

```json
{
    "id": score,
    ...
}
```

```
    ```
    """
```

```
            "evaluation_criteria": "..."
        }
    ]
    """
```

**Prompt for Evaluation Criteria Generation**

We generate evaluation questions and scoring criteria initially using the GPT-4o API with a fixed temperature of 0.1 to ensure score stability. Due to performance degradation in GPT-4o when handling long contexts, we have separated the prompts for generating questions and assigning weights. This approach ensures that GPT-4o can fully adhere to all the key points specified in each prompt. These outputs are then carefully reviewed and refined by human annotators to ensure they align with human judgment. The prompt we used is as follows:

**Prompt for Evaluation Criteria Generation**

```
IMAGINE_IMAGE = """
This test case is designed to evaluate the image
↪   generation model. What do you think the correct
↪   image should look like based on this prompt?
Prompt: [PROMPT]
Expected: [EXPECTED]
"""


DESIGN_EVALUATION_QUESTIONS = """
Now, create a set of evaluation questions to determine
↪   whether the image is accurate.
For each question, define the criteria for different
↪   levels of performance, with the rating scale
↪   ranging from [0, 1].

Prompt: [PROMPT]
Expected: [EXPECTED]
"""


WEIGHT = """
# Image Generation Model Assessment

This prompt is designed to evaluate the performance of
↪   an image generation model.

Prompt: [PROMPT]
Reference Answer: [EXPECTED]
Assessment Points: [ASSESSMENT POINTS]


---


### Weight Assignment Instructions

- Based on key evaluation criteria, assign weights
↪   (1-10) to each evaluation question.
- Higher weights should be assigned to critical
↪   factors related to **core reasoning points**.
- Mid-range weights should be assigned to aspects that
↪   are not related to reasoning but are still
↪   relevant to the image.
- Lower weights should be assigned to aspects like
↪   **image quality**, **realism**, and **clarity**.


---


### Evaluation Questions

Please provide the **complete list of evaluation
↪   questions** without any omissions.


```json
[
    {
        "id": "number",
        "weight": "weight",
        "question": "...",
```

| Mathematical Reasoning | Description |
|---|---|
| Mathematical Function Visualization (12.50%) | Mathematical Function Visualization involves generating clear and informative images that depict *mathematical functions*, their *properties*, and the *relationships* between various *mathematical entities*, such as *variables* and *parameters*. |
| Vector & Matrix Visualization (12.50%) | Vector & Matrix Visualization involves understanding and illustrating *vectors*, *matrices*, and *transformations* in *geometrical space*. |
| Combinatorial Reasoning (12.50%) | Combinatorial Reasoning involves depicting *permutations*, *combinations*, or *arrangements* of *objects*, often within a *geometric* or *graphical context*. |
| Set Theory & Relations (12.50%) | Set Theory & Relations involves representing *sets*, *subsets*, and their *relations* in visual forms (e.g., using *Venn diagrams* or *set-builder notation*). |
| Cryptographic & Encoding Reasoning (12.50%) | Cryptographic & Encoding Reasoning involves rendering *encrypted texts*, *ciphers*, or *encoding schemes* (e.g., *Morse code*, *binary representations*). |
| Number Theory (12.50%) | Number Theory Visualization involves depicting *prime numbers*, *divisibility rules*, and other abstract *mathematical concepts*. |
| Geometrical Transformations (12.50%) | Geometrical Transformations involves illustrating *symmetry operations* like *rotations*, *reflections*, *translations*, or *dilations* in space. |
| Spatial Reasoning (12.50%) | Spatial Reasoning refers to the ability to reason and infer the correct *geometric configuration* of *objects*, such as *lines* and *shapes*, in a defined space, based on specified *spatial relationships*. |

Table 6: Definitions and proportions of the eight subcategories in mathematical reasoning within `R2I-Bench`. The percentage indicates the proportion of each subcategory within the overall mathematical category.

| Concept Mixing Reasoning | Description |
|---|---|
| Functional Mixing (44.44%) | Functional mixing includes creating new *concepts* that involve blending different *functional properties* of *objects*. |
| Literal Mixing (55.56%) | Literal Mixing Reasoning combines *elements* from different *concepts* in a *straightforward*, *literal* manner, such as merging *objects* or *creatures*. |

Table 7: Definitions and proportions of the two subcategories in concept mixing reasoning within `R2I-Bench`. The percentage indicates the proportion of each subcategory within the overall concept mixing category.

| Causal Reasoning | Description |
|---|---|
| Cause to Effect Reasoning (52.98%) | Given a *cause*, generate an *image* depicting the *effect*. |
| Effect to Cause Reasoning (47.02%) | Given an *effect*, generate an *image* depicting the possible *cause*. |

Table 8: Definitions and proportions of the two subcategories in causal reasoning within `R2I-Bench`. The percentage indicates the proportion of each subcategory within the overall causal category.

| Compositional Reasoning | Description |
|---|---|
| Creative Composition Reasoning (32.15%) | Creative compositional reasoning is the ability to combine different *ideas* or *objects* in *innovative* and *imaginative* ways to create *novel* and *unique scenes* that have not been seen before. |
| Inferential Spatial Reasoning (32.15%) | Inferential spatial reasoning refers to the ability to determine the *positions* or *size relationships* between *objects* without explicit descriptions. |
| Prescriptive Spatial Reasoning (35.69%) | Prescriptive Spatial Reasoning refers to the ability to follow clear *instructions* about where *objects* should be placed in a scene, ensuring the layout matches the described *relationships*. Understanding phrases like *"left of", "above", "inside"*. |

Table 9: Definitions and proportions of the three subcategories in compositional reasoning within `R2I-Bench`. The percentage indicates the proportion of each subcategory within the overall compositional reasoning category.

| Logical Reasoning | Description |
|---|---|
| Categorical Reasoning (11.90%) | Categorical reasoning involves determining whether a specific *concept* belongs to a particular *category*. This type of reasoning often involves *quantifiers* such as *"all,", "everyone,", "any,", "no,"* and *"some."* |
| Hypothetical Reasoning (11.90%) | Hypothetical reasoning is the process of using a *systematic*, *structured* approach to analyze *information*, draw *conclusions*, and solve *problems* based on given *premises* or *conditions*. |
| Disjunctive Reasoning (16.51%) | Disjunctive reasoning involves *premises* in the form *"either ... or ..."*, where the *conclusion* holds as long as one *premise* is true. |
| Conjunctive Reasoning (16.51%) | Conjunctive reasoning involves *premises* in the form *"both ... and ..."*, where the *conclusion* holds only if all the *premises* is true. |
| Sufficient Conditional Reasoning (13.49%) | Sufficient Conditional Reasoning is based on *conditional statements* of the form *"If P, then Q"*, in which P is the *antecedent* and Q is the *consequent*. |
| Deductive Reasoning (13.97%) | Deductive reasoning focuses on deriving specific *conclusions* from general *principles* or *premises*, ensuring that *conclusions* logically follow if the *premises* are true. |
| Abductive Reasoning (16.03%) | Abductive reasoning, considered more *creative* and *open-ended*, involves forming *hypotheses* to explain *observations*, often generating the most *plausible explanation* rather than a *guaranteed conclusion*. |

Table 10: Definitions and proportions of the seven subcategories in logical reasoning within `R2I-Bench`. The percentage indicates the proportion of each subcategory within the overall logical reasoning category.

| Numerical Reasoning | Description |
|---|---|
| Exact Number Generation (31.06%) | Exact number generation examines the model's ability to correctly generate an *exact number* of *objects*. |
| Approximate Number Generation and Zero (31.37%) | Approximate number generation evaluates models on their ability to correctly depict *entities* with quantities expressed in *approximate terms* by means of *linguistic quantifiers(e.g., "many", "a few", or "more")*. |
| Conceptual Quantitative Reasoning (37.58%) | Conceptual quantitative reasoning evaluates models on prompts that require a *conceptual understanding* of *objects* and their *parts*. |

Table 11: Definitions and proportions of the three subcategories in Numerical reasoning within `R2I-Bench`. The percentage indicates the proportion of each subcategory within the overall Numerical reasoning category.

| Commonsense Reasoning | Description |
|---|---|
| Affordance (14.53%) | Affordance commonsense reasoning involves providing a description of an object's potential *use* or *function*, requiring the model to generate an object based on that description. |
| Attribute (14.53%) | Attribute commonsense reasoning refers to the model's ability to infer or recognize the *properties* and *characteristics* of an object, utilizing both observable and unobservable information. |
| Color (14.82%) | Color commonsense reasoning pertains to the model's ability to infer the correct *color* of an object based on commonsense knowledge related to *color*. |
| Emotion Intention Commonsense (11.94%) | Emotion intention commonsense reasoning explores the model's ability to understand *emotional cues* and *intentions*, particularly in the context of *human-object interactions* in images. This subcategory evaluates how well the model can recognize and interpret *emotional states* and *intentions* from visual input. |
| Social & Cultural Knowledge (Object) (14.68%) | Social and cultural commonsense reasoning (Object) assesses the model's ability to leverage knowledge related to *social* and *cultural contexts* when generating a specific object. |
| Social & Cultural Knowledge (Scene) (15.11%) | Social and cultural commonsense reasoning (Scene) evaluates the model's ability to incorporate knowledge of *social* and *cultural contexts* when generating *scenes* or *environments* that accurately reflect specific *social* and *cultural* settings. |
| Temporal Understanding (14.39%) | Temporal understanding commonsense reasoning focuses on the model's ability to infer and apply knowledge related to *time-dependent changes* or *events*, including the ability to predict how *objects* or *scenes* may evolve over time based on contextual and temporal understanding. |

Table 12: Definitions and proportions of the seven subcategories in commonsense reasoning within `R2I-Bench`. The percentage indicates the proportion of each subcategory within the overall commonsense reasoning category.
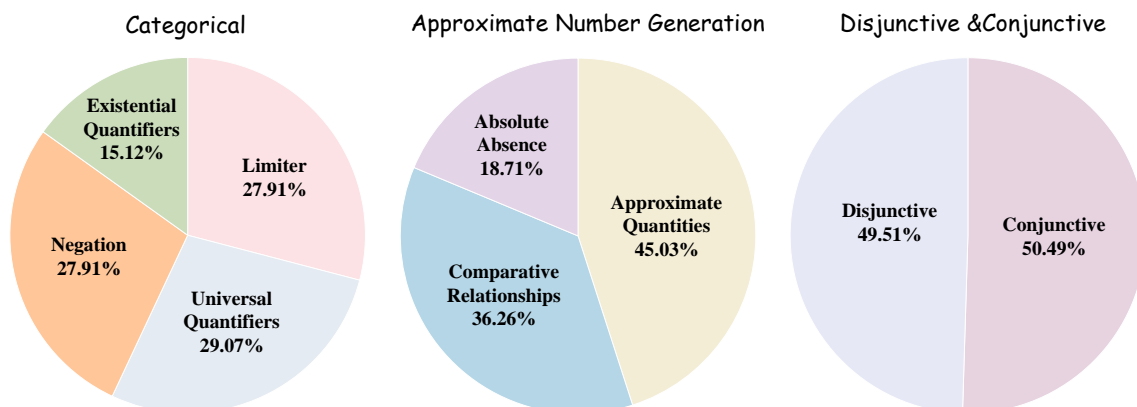


Figure 8: **Distribution of Quantifiers and Operations in Categorical, Approximate Number Generation, Disjunctive Reasoning, and Conjunctive Reasoning.**
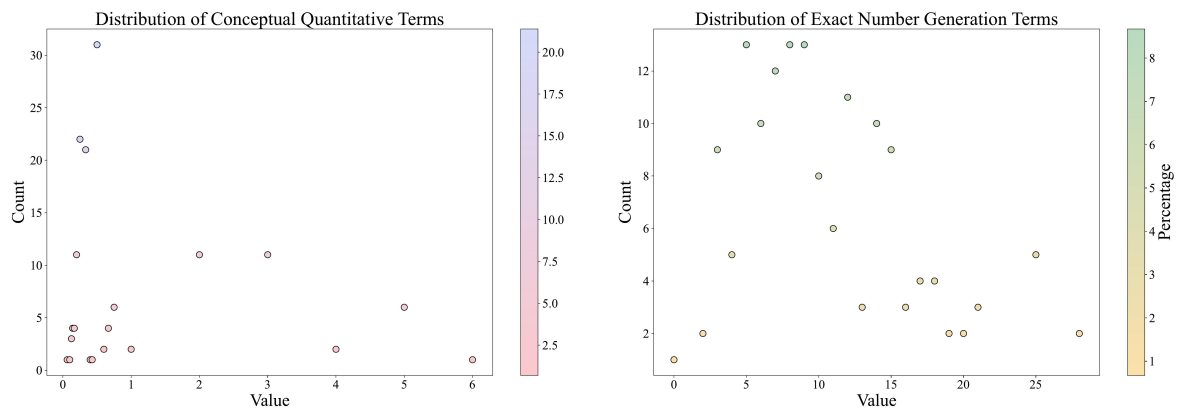
Figure 9: **Distribution of Numbers in Exact Number Generation and Conceptual Quantitative Reasoning.** Due to the current limitations of the best visual language models in numerical tasks, the numbers in Exact Number Generation are restricted to values within 30.

## B  Experiment Details

All experiments with open-source models are performed on A-40 GPUs, whereas experiments involving closed-source models are conducted using the API key provided by the respective service. All experiments are conducted in a zero-shot setting to assess the generalization capabilities of text-to-image (T2I) generation models on reasoning tasks, without relying on few-shot prompting or additional fine-tuning.

**Model Details**   For different T2I models, we select their latest models and best-performing configurations for evaluation to fully `R2I-Bench` their reasoning ability. Table 15 presents the release time and model sources of T2I models used in `R2I-Bench`.

**Comparing Auto-Evaluators on Relevant Dimensions**   Table 13 reports the performance of all evaluated models with respect to *textual alignment*, *reasoning accuracy*, and *image quality*. This separation highlights the strengths and weaknesses of different models beyond the overall score.

### B.1   Main Results across 33 Subcategories

Table 16 to 20 are the main results of the models across subcategories in *Mathematical Reasoning, Logical Reasoning, Commonsense Reasoning, Concept Mixing Reasoning, Causal Reasoning, Numerical Reasoning and Compositional Reasoning*. Table 14 reports overall performance with standard errors (SE) and 95% confidence intervals (CIs).

Table 13: Comparison of auto-evaluators across textual alignment (TA), reasoning accuracy (RA), and image quality (IQ).

| Model | TA | RA | IQ |
|---|---|---|---|
| SD3-medium | 0.48 | 0.40 | 0.42 |
| Lumina-Image2.0 | 0.50 | 0.41 | 0.43 |
| Sana-1.5 | 0.52 | 0.41 | 0.43 |
| Lumina-T2I | 0.45 | 0.32 | 0.40 |
| Omnigen | 0.48 | 0.35 | 0.44 |
| LLM4GEN$_{SD1.5}$ | 0.46 | 0.35 | 0.42 |
| ELLA$_{SD1.5}$ | 0.37 | 0.25 | 0.32 |
| EMU3 | 0.51 | 0.36 | 0.43 |
| Janus-Pro-7B | 0.47 | 0.35 | 0.40 |
| LlamaGen | 0.35 | 0.25 | 0.31 |
| Show-o | 0.38 | 0.34 | 0.33 |
| Show-o+ORM | 0.33 | 0.35 | 0.33 |
| Show-o+DPO | 0.38 | 0.36 | 0.37 |
| Show-o+PARM | 0.42 | 0.38 | 0.40 |
| DALL-E-3 | 0.65 | 0.62 | 0.48 |
| gpt-image-1 | 0.65 | 0.72 | 0.50 |
| gpt-4+SD3-medium | 0.70 | 0.59 | 0.43 |

### B.2   Human Annotators

To incorporate human judgment and validate the effectiveness of our evaluation approach, we organize a group of senior college students. Each participant is tasked with comparing the image outputs generated by two similarly performing models, `Lumina-Image 2.0` and `Sana-1.5`, selecting the image they find most aligned with the prompt or indicating if both outputs are equally satisfactory or unsatisfactory.

Table 14: Main results with standard errors (SE) and 95% confidence intervals (CIs).

| Model | Overall | SE | 95% CI |
|---|---|---|---|
| SD3-medium | 0.45 | 0.03 | [0.42, 0.48] |
| Lumina-Image 2.0 | 0.42 | 0.02 | [0.40, 0.44] |
| Sana-1.5 | 0.41 | 0.03 | [0.38, 0.44] |
| Lumina-T2I | 0.33 | 0.04 | [0.29, 0.37] |
| Omnigen | 0.40 | 0.02 | [0.38, 0.42] |
| LLM4GEN$_{SD1.5}$ | 0.40 | 0.03 | [0.37, 0.43] |
| ELLA$_{SD1.5}$ | 0.31 | 0.03 | [0.28, 0.34] |
| EMU3 | 0.41 | 0.02 | [0.39, 0.43] |
| Janus-Pro-7B | 0.38 | 0.03 | [0.35, 0.41] |
| LlamaGen | 0.29 | 0.03 | [0.26, 0.32] |
| Show-o | 0.36 | 0.02 | [0.34, 0.38] |
| Show-o+ORM | 0.34 | 0.03 | [0.31, 0.37] |
| Show-o+DPO | 0.36 | 0.02 | [0.34, 0.38] |
| Show-o+PARM | 0.38 | 0.02 | [0.36, 0.40] |
| DALL-E-3 | 0.71 | 0.02 | [0.69, 0.73] |
| gpt-image-1 | 0.77 | 0.01 | [0.75, 0.79] |
| gpt-4o-SD3-medium | 0.58 | 0.02 | [0.56, 0.60] |

### B.3   Image by Categories

This section presents examples of images from various categories in `R2I-Bench`. Figure 12 to 16 coresponding to images under the categories of *Commonsense Reasoning, Numerical Reasoning, Causal Reasoning, Logical Reasoning, Mathemati-*

*cal Reasoning, Concept Mixing Reasoning, Compositional Reasoning*, respectively.

## B.4 Comparison of Subcategory Performance: Standard T2I Model vs. Pipeline-based Framework

Figure 10 presents detailed performance comparison: standard T2I model vs. pipeline-based framework
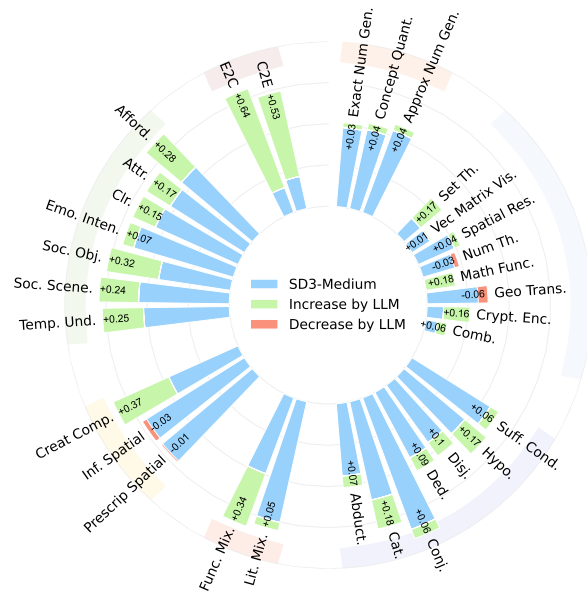


Figure 10: **Detailed Performance Comparison: Standard T2I Model vs. Pipeline-based Framework**. We denote the results of standard T2I models in blue pillars and highlight the increase and decrease magnitude with the pipeline-based framework by green and red colors, respectively.
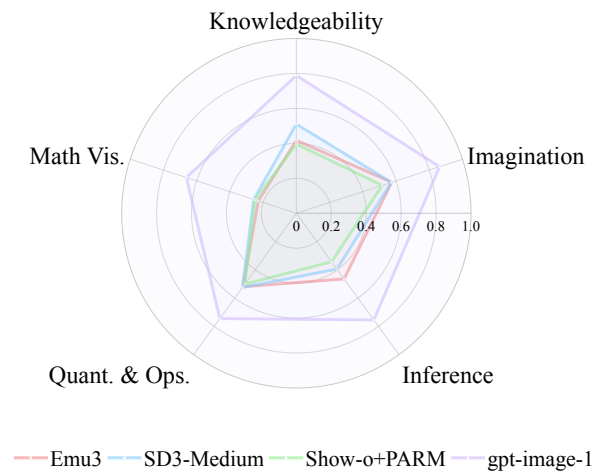


Figure 11: Performance of the top models across four different architectures on five reasoning abilities.

## B.5 Results of Our Evaluation Methods and Additional Metrics in the Benchmark

In this section, we present the results of the evaluation methods employed, along with other metrics. The detailed evaluation results are provided in Table 21.

## B.6 Quantitative and Qualitative Analysis of `Nano-Banana`

Recently, `Nano-Banana` (Team, 2025) has demonstrated state-of-the-art performance in image generation and editing, which motivates us to further evaluate it on R2I-Bench. As `Nano-Banana` is a closed-source model with API access requiring paid credits, we manually sampled 10 T2I prompts from each of the seven reasoning categories in R2I-Bench for testing. Table 22 reports its performance across these categories, where we find that `Nano-Banana` performs noticeably less competitively compared to both `DALLE-3` and `GPT-Image-1`. In addition, Figure 19 provides detailed qualitative examples to illustrate its reasoning limitations. Overall, these results highlight that image generation remains an unsolved problem, especially in reasoning-driven scenarios, and demonstrate the key contribution of `R2I-Bench` to this field.

Table 15: **The Release Time and Model Source of T2I Models Evaluated in** `R2I-Bench`.

| Model | Release Time | Source | URL |
|---|---|---|---|
| EMU3 (Wang et al., 2024) | 2024-09 | local checkpoint | https://github.com/baaivision/Emu3 |
| Janus-Pro-7B (Chen et al., 2025) | 2025-01 | local checkpoint | https://github.com/deepseek-ai/Janus/ |
| LlamaGen (Sun et al., 2024a) | 2024-06 | local checkpoint | https://huggingface.co/FoundationVision/LlamaGen |
| SD3-medium (Esser et al., 2024) | 2024-10 | local checkpoint | https://huggingface.co/stabilityai/stable-diffusion-3.5-medium |
| Lumina-Image-2.0 (Qin et al., 2025) | 2025-03 | local checkpoint | https://github.com/Lumina-Image2.0 |
| Sana-1.5 (Xie et al., 2025a) | 2025-03 | local checkpoint | https://github.com/NVlabs/Sana |
| Lumina-T2I (Qin et al., 2025) | 2024-05 | local checkpoint | https://huggingface.co/Alpha-VLLM/Lumina-Next-SFT-diffusers |
| LLM4GEN$_{SD1.5}$ (Liu et al., 2025) | 2024-07 | local checkpoint | https://github.com/YUHANG-Ma/LLM4GEN |
| ELLA$_{SD1.5}$ (Hu et al., 2024) | 2024-03 | local checkpoint | https://github.com/TencentQQGYLab/ELLA |
| Show-o+PARM (Zhang et al., 2025) | 2025-01 | local checkpoint | https://huggingface.co/ZiyuG/Image-Generation-CoT |
| Show-o+DPO (Zhang et al., 2025) | 2025-01 | local checkpoint | https://huggingface.co/ZiyuG/Image-Generation-CoT |
| Show-o+ORM (Zhang et al., 2025) | 2025-01 | local checkpoint | https://huggingface.co/ZiyuG/Image-Generation-CoT |
| GPT-4o (Hurst et al., 2024) | 2025-04 | GPT-Image-1 | https://platform.openai.com/ |
| nano-banana (Team, 2025) | 2025-08 | nano-banana | https://aistudio.google.com/ |

| Method | Overall | Comb. | Crypt. Enc. | Geo. Trans. | Math Func. | Num. Th. | Spatial Reas. | Vec/Mat. Vis. | Set Th. |
|---|---|---|---|---|---|---|---|---|---|
| *Diffusion Models* | | | | | | | | | |
| SD3-medium (Esser et al., 2024) | 0.19 | 0.07 | 0.10 | 0.37 | 0.01 | 0.23 | 0.24 | 0.13 | 0.13 |
| Lumina-Image 2.0 (Qin et al., 2025) | 0.13 | 0.09 | 0.09 | 0.18 | 0.03 | 0.06 | 0.28 | 0.01 | 0.16 |
| Sana-1.5 (Xie et al., 2025a) | 0.13 | 0.10 | 0.06 | 0.32 | 0.02 | 0.08 | 0.16 | 0.06 | 0.16 |
| Lumina-T2I (Qin et al., 2025) | 0.13 | 0.04 | 0.01 | 0.17 | 0.03 | 0.07 | 0.16 | 0.05 | 0.07 |
| OminGen (Xiao et al., 2024) | 0.18 | 0.19 | 0.05 | 0.27 | 0.06 | 0.33 | 0.26 | 0.08 | 0.21 |
| LLM4GEN$_{SD1.5}$ (Liu et al., 2025) | 0.07 | 0.03 | 0.01 | 0.16 | 0.01 | 0.01 | 0.01 | 0.01 | 0.09 |
| ELLA$_{SD1.5}$ (Hu et al., 2024) | 0.07 | 0.01 | 0.03 | 0.14 | 0.01 | 0.01 | 0.11 | 0.07 | 0.07 |
| *AutoRegressive Models* | | | | | | | | | |
| EMU3 (Wang et al., 2024) | 0.09 | 0.05 | 0.01 | 0.18 | 0.03 | 0.08 | 0.14 | 0.05 | 0.08 |
| Janus-Pro-7B (Chen et al., 2025) | 0.07 | 0.02 | 0.01 | 0.16 | 0.02 | 0.06 | 0.12 | 0.01 | 0.06 |
| LlamaGen (Sun et al., 2024a) | 0.07 | 0.04 | 0.01 | 0.24 | 0.01 | 0.01 | 0.01 | 0.05 | 0.10 |
| Show-o (Xie et al., 2025b) | 0.12 | 0.12 | 0.02 | 0.20 | 0.01 | 0.26 | 0.19 | 0.03 | 0.14 |
| *Reasoning-Enhanced Models* | | | | | | | | | |
| Show-o+ORM (Zhang et al., 2025) | 0.12 | 0.12 | 0.02 | 0.19 | 0.02 | 0.24 | 0.18 | 0.04 | 0.13 |
| Show-o+DPO (Zhang et al., 2025) | 0.13 | 0.14 | 0.04 | 0.20 | 0.03 | 0.23 | 0.20 | 0.06 | 0.14 |
| Show-o+PARM (Zhang et al., 2025) | 0.13 | 0.13 | 0.03 | 0.21 | 0.02 | 0.27 | 0.20 | 0.04 | 0.15 |
| *Close Source Models* | | | | | | | | | |
| DALL-E3 (OpenAI, 2023) | 0.21 | 0.07 | 0.14 | 0.32 | 0.05 | 0.18 | 0.42 | 0.12 | 0.36 |
| gpt-image-1 (Hurst et al., 2024) | 0.58 | 0.43 | 0.43 | 0.73 | 0.59 | 0.49 | 0.74 | 0.46 | 0.75 |

Table 16: Evaluation of mathematical capabilities in generative models. Comb.: Combinatorial, Crypt. Enc.: Cryptographic Encoding, Geo. Trans.: Geometrical Transformations, Math Func.: Mathematical Function, Num. Th.: Number Theory, Spatial Reas.: Spatial Reasoning, Vec/Mat. Vis.: Vector & Matrix Visualization, Set Th.: Set Theory.

| Method | Overall | Abduc. | Cat. | Conj. | Ded. | Disj. | Hypo. | Suff. |
|---|---|---|---|---|---|---|---|---|
| *Diffusion Models* | | | | | | | | |
| SD3-medium (Esser et al., 2024) | 0.55 | 0.44 | 0.61 | 0.85 | 0.45 | 0.43 | 0.48 | 0.56 |
| Lumina-Image 2.0 (Qin et al., 2025) | 0.56 | 0.44 | 0.57 | 0.87 | 0.38 | 0.51 | 0.52 | 0.54 |
| Sana-1.5 (Xie et al., 2025a) | 0.49 | 0.46 | 0.56 | 0.89 | 0.50 | 0.48 | 0.59 | 0.56 |
| Lumina-T2I (Qin et al., 2025) | 0.38 | 0.33 | 0.50 | 0.69 | 0.54 | 0.43 | 0.55 | 0.53 |
| OminGen (Xiao et al., 2024) | 0.51 | 0.42 | 0.64 | 0.69 | 0.39 | 0.52 | 0.41 | 0.47 |
| LLM4GEN$_{SD1.5}$ (Liu et al., 2025) | 0.55 | 0.33 | 0.48 | 0.70 | 0.40 | 0.53 | 0.55 | 0.49 |
| ELLA$_{SD1.5}$ (Hu et al., 2024) | 0.40 | 0.29 | 0.41 | 0.64 | 0.26 | 0.59 | 0.40 | 0.39 |
| *AutoRegressive Models* | | | | | | | | |
| EMU3 (Wang et al., 2024) | 0.55 | 0.38 | 0.53 | 0.71 | 0.44 | 0.64 | 0.52 | 0.58 |
| Janus-Pro-7B (Chen et al., 2025) | 0.46 | 0.25 | 0.64 | 0.85 | 0.13 | 0.57 | 0.52 | 0.22 |
| LlamaGen (Sun et al., 2024a) | 0.38 | 0.15 | 0.48 | 0.55 | 0.17 | 0.59 | 0.29 | 0.35 |
| Show-o (Xie et al., 2025b) | 0.42 | 0.40 | 0.62 | 0.71 | 0.35 | 0.42 | 0.32 | 0.38 |
| *Reasoning-Enhanced Models* | | | | | | | | |
| Show-o+ORM (Zhang et al., 2025) | 0.37 | 0.33 | 0.48 | 0.47 | 0.35 | 0.41 | 0.37 | 0.17 |
| Show-o+DPO (Zhang et al., 2025) | 0.41 | 0.29 | 0.44 | 0.44 | 0.36 | 0.43 | 0.34 | 0.18 |
| Show-o+PARM (Zhang et al., 2025) | 0.45 | 0.38 | 0.53 | 0.76 | 0.33 | 0.45 | 0.31 | 0.36 |
| *Close Source Models* | | | | | | | | |
| DALLE (OpenAI, 2023) | 0.69 | 0.56 | 0.67 | 0.87 | 0.70 | 0.46 | 0.79 | 0.78 |
| gpt-image-1 (OpenAI, 2023) | 0.81 | 0.79 | 0.88 | 0.95 | 0.79 | 0.76 | 0.79 | 0.73 |

Table 17: Evaluation of text-to-image generation on Logical Reasoning in `R2I-Bench`. Abduc.: Abductive, Cat.: Categorical, Conj.: Conjunctive, Ded.: Deductive, Disj.: Disjunctive, Hypo.: Hypothetical, Suff.: Sufficient Conditional

| Method | Overall | Afford. | Attribute | Color | Emotion | Object | Scene | Temp. |
|---|---|---|---|---|---|---|---|---|
| *Diffusion Models* | | | | | | | | |
| SD3-medium (Esser et al., 2024) | 0.54 | 0.56 | 0.53 | 0.55 | 0.63 | 0.44 | 0.55 | 0.52 |
| Lumina-Image 2.0 (Qin et al., 2025) | 0.49 | 0.46 | 0.53 | 0.51 | 0.65 | 0.34 | 0.53 | 0.46 |
| Sana-1.5 (Xie et al., 2025a) | 0.49 | 0.42 | 0.60 | 0.51 | 0.64 | 0.33 | 0.53 | 0.51 |
| Lumina-T2I (Qin et al., 2025) | 0.38 | 0.36 | 0.47 | 0.40 | 0.57 | 0.33 | 0.46 | 0.39 |
| OminGen (Xiao et al., 2024) | 0.43 | 0.41 | 0.51 | 0.39 | 0.54 | 0.30 | 0.47 | 0.41 |
| LLM4GEN$_{SD1.5}$ (Liu et al., 2025) | 0.55 | 0.37 | 0.47 | 0.44 | 0.66 | 0.36 | 0.56 | 0.51 |
| ELLA$_{SD1.5}$ (Hu et al., 2024) | 0.40 | 0.33 | 0.40 | 0.34 | 0.37 | 0.28 | 0.36 | 0.32 |
| *AutoRegressive Models* | | | | | | | | |
| EMU3 (Wang et al., 2024) | 0.46 | 0.40 | 0.50 | 0.43 | 0.58 | 0.39 | 0.52 | 0.42 |
| Janus-Pro-7B (Chen et al., 2025) | 0.45 | 0.38 | 0.57 | 0.45 | 0.58 | 0.32 | 0.49 | 0.40 |
| LlamaGen (Sun et al., 2024a) | 0.38 | 0.38 | 0.42 | 0.39 | 0.40 | 0.29 | 0.38 | 0.38 |
| Show-o (Xie et al., 2025b) | 0.42 | 0.44 | 0.48 | 0.41 | 0.44 | 0.32 | 0.44 | 0.36 |
| *Reasoning-Enhanced Models* | | | | | | | | |
| Show-o+ORM (Zhang et al., 2025) | 0.42 | 0.42 | 0.49 | 0.40 | 0.47 | 0.35 | 0.47 | 0.38 |
| Show-o+DPO (Zhang et al., 2025) | 0.43 | 0.43 | 0.52 | 0.44 | 0.45 | 0.36 | 0.47 | 0.36 |
| Showo-o+PARM (Zhang et al., 2025) | 0.45 | 0.45 | 0.48 | 0.46 | 0.55 | 0.40 | 0.49 | 0.47 |
| *Close Source Models* | | | | | | | | |
| DALLE3 (OpenAI, 2023) | 0.78 | 0.70 | 0.80 | 0.86 | 0.81 | 0.81 | 0.77 | 0.72 |
| gpt-iamge-1 (OpenAI, 2023) | 0.83 | 0.89 | 0.79 | 0.80 | 0.89 | 0.85 | 0.87 | 0.75 |

Table 18: Evaluation Results of text-to-image generation on Commonsense Reasoning in `R2I-Bench`. Afford.: Affordance. Temp.: Temporal Understanding. Emotion: Emotion Intention Commonsense Reasoning. Object: Social Cultural Knowledge (Object). Scene: Social Cultural Knowledge (Scene).

| Method | Overall | Numerical | | | Overall | Causal Reasoning | |
|---|---|---|---|---|---|---|---|
| | | Approx. | Conceptual. | Exact. | | C2E | E2C |
| *Diffusion Models* | | | | | | | |
| SD3-medium (Esser et al., 2024) | 0.50 | 0.53 | 0.49 | 0.48 | 0.18 | 0.20 | 0.16 |
| Lumina-Image 2.0 (Qin et al., 2025) | 0.43 | 0.54 | 0.40 | 0.35 | 0.40 | 0.37 | 0.44 |
| Sana-1.5 (Xie et al., 2025a) | 0.47 | 0.58 | 0.37 | 0.47 | 0.21 | 0.23 | 0.19 |
| Lumina-T2I (Qin et al., 2025) | 0.45 | 0.53 | 0.45 | 0.38 | 0.18 | 0.18 | 0.18 |
| OminGen (Xiao et al., 2024) | 0.47 | 0.59 | 0.40 | 0.42 | 0.34 | 0.26 | 0.41 |
| LLM4GEN$_{SD1.5}$ (Liu et al., 2025) | 0.39 | 0.44 | 0.36 | 0.36 | 0.45 | 0.46 | 0.44 |
| ELLA$_{SD1.5}$ (Hu et al., 2024) | 0.32 | 0.41 | 0.25 | 0.30 | 0.29 | 0.22 | 0.38 |
| *AutoRegressive Models* | | | | | | | |
| EMU3 (Wang et al., 2024) | 0.61 | 0.73 | 0.54 | 0.56 | 0.41 | 0.36 | 0.47 |
| Janus-Pro-7B (Chen et al., 2025) | 0.46 | 0.53 | 0.38 | 0.48 | 0.36 | 0.34 | 0.39 |
| LlamaGen (Sun et al., 2024a) | 0.35 | 0.43 | 0.31 | 0.30 | 0.12 | 0.12 | 0.12 |
| Show-o (Xie et al., 2025b) | 0.57 | 0.68 | 0.50 | 0.53 | 0.30 | 0.23 | 0.38 |
| *Reasoning-Enhanced Models* | | | | | | | |
| Show-o+ORM (Zhang et al., 2025) | 0.49 | 0.52 | 0.46 | 0.49 | 0.26 | 0.30 | 0.23 |
| Show-o+DPO (Zhang et al., 2025) | 0.51 | 0.58 | 0.46 | 0.50 | 0.31 | 0.35 | 0.28 |
| Show-o+PARM (Zhang et al., 2025) | 0.56 | 0.65 | 0.49 | 0.53 | 0.32 | 0.36 | 0.27 |
| *Close Source Models* | | | | | | | |
| DALLE (OpenAI, 2023) | 0.69 | 0.71 | 0.64 | 0.72 | 0.64 | 0.69 | 0.59 |
| gpt-image-1 (Hurst et al., 2024) | 0.88 | 0.90 | 0.81 | 0.92 | 0.71 | 0.85 | 0.56 |

Table 19: Evaluation of text-to-image generation on Numerical Reasoning and Causal Reasoning in `R2I-Bench`. Approx.: Approximate Number Generation. Conceptual: Conceptual Quantitative Reasoning. Exact: Exact Number Generation. C2E: Cause to Effect Reasoning. E2C: Effect to Cause Reasoning.

| Method | Overall | Concept Mixing | | Overall | Compositional | | |
|---|---|---|---|---|---|---|---|
| | | Functional | Literal | | Creative | Inferential | Prescriptive |
| *Diffusion Models* | | | | | | | |
| SD3-medium (Esser et al., 2024) | 0.63 | 0.49 | 0.75 | 0.64 | 0.46 | 0.73 | 0.72 |
| Lumina-Image 2.0 (Qin et al., 2025) | 0.54 | 0.52 | 0.56 | 0.65 | 0.50 | 0.72 | 0.73 |
| Sana-1.5 (Xie et al., 2025a) | 0.66 | 0.55 | 0.75 | 0.67 | 0.59 | 0.79 | 0.63 |
| Lumina-T2I (Qin et al., 2025) | 0.55 | 0.47 | 0.62 | 0.49 | 0.42 | 0.56 | 0.49 |
| Omnigen (Xiao et al., 2024) | 0.43 | 0.27 | 0.58 | 0.60 | 0.46 | 0.80 | 0.54 |
| LLM4GEN$_{SD1.5}$ (Liu et al., 2025) | 0.60 | 0.48 | 0.70 | 0.48 | 0.44 | 0.61 | 0.39 |
| ELLA$_{SD1.5}$ (Hu et al., 2024) | 0.40 | 0.33 | 0.46 | 0.44 | 0.34 | 0.55 | 0.43 |
| *AutoRegressive Models* | | | | | | | |
| EMU3 (Wang et al., 2024) | 0.62 | 0.51 | 0.70 | 0.59 | 0.50 | 0.68 | 0.59 |
| Janus-Pro-7B (Chen et al., 2025) | 0.64 | 0.55 | 0.71 | 0.60 | 0.56 | 0.73 | 0.52 |
| LlamaGen (Sun et al., 2024a) | 0.49 | 0.45 | 0.53 | 0.39 | 0.42 | 0.50 | 0.27 |
| Show-o (Xie et al., 2025b) | 0.56 | 0.42 | 0.68 | 0.55 | 0.41 | 0.65 | 0.60 |
| *Reasoning-Enhanced Models* | | | | | | | |
| Show-o+ORM (Zhang et al., 2025) | 0.44 | 0.30 | 0.56 | 0.45 | 0.35 | 0.54 | 0.45 |
| Show-o+DPO (Zhang et al., 2025) | 0.48 | 0.35 | 0.61 | 0.47 | 0.38 | 0.56 | 0.47 |
| Show-o+PARM (Zhang et al., 2025) | 0.51 | 0.37 | 0.63 | 0.49 | 0.39 | 0.58 | 0.51 |
| *Close Source Models* | | | | | | | |
| DALLE3 (OpenAI, 2023) | 0.86 | 0.82 | 0.90 | 0.76 | 0.73 | 0.82 | 0.72 |
| gpt-image-1 (Hurst et al., 2024) | 0.89 | 0.88 | 0.90 | 0.87 | 0.81 | 0.84 | 0.95 |

Table 20: Evaluation of text-to-image generation on Concept Mixing and Compositional Reasoning in `R2I-Bench`. Functional: Functional Mixing Reasoning. Literal: Literal Mixing Reasoning. Creative: Creative Compositional Reasoning. Inferential: Inferential Spatial Reasoning. Prescriptive: Prescriptive Spatial Reasoning

Table 21: Comparison of our evaluation methods and other image-text alignment metrics across different models and categories.

| Category | Models | Pairwise Accuracy ↑ | Kendall's $\tau$ ↑ | Spearman's Rank Correlation ↑ |
|---|---|---|---|---|
| Commonsense | CLIPScore (Hessel et al., 2021) | 0.61 | 0.22 | 0.42 |
| | DSGScore (Cho et al., 2024) | 0.54 | 0.10 | 0.30 |
| | VIEScore (Ku et al., 2024) | 0.70 | 0.45 | 0.34 |
| | VQAscore (Lin et al., 2024) | 0.60 | 0.22 | 0.39 |
| | Ours | 0.64 | 0.60 | 0.62 |
| Compositional | CLIPScore (Hessel et al., 2021) | 0.71 | 0.42 | 0.39 |
| | DSGScore (Cho et al., 2024) | 0.50 | 0.38 | 0.26 |
| | VIEScore (Ku et al., 2024) | 0.58 | 0.40 | 0.32 |
| | VQAscore (Lin et al., 2024) | 0.64 | 0.48 | 0.45 |
| | Ours | 0.73 | 0.76 | 0.61 |
| Logical | CLIPScore (Hessel et al., 2021) | 0.61 | 0.22 | 0.30 |
| | DSGScore (Cho et al., 2024) | 0.63 | 0.15 | 0.25 |
| | VIEScore (Ku et al., 2024) | 0.78 | 0.63 | 0.40 |
| | VQAscore (Lin et al., 2024) | 0.76 | 0.72 | 0.68 |
| | Ours | 0.76 | 0.72 | 0.63 |
| Causal | CLIPScore (Hessel et al., 2021) | 0.54 | 0.18 | 0.21 |
| | DSGScore (Cho et al., 2024) | 0.51 | 0.22 | 0.28 |
| | VIEScore (Ku et al., 2024) | 0.69 | 0.64 | 0.68 |
| | VQAscore (Lin et al., 2024) | 0.62 | 0.33 | 0.70 |
| | Ours | 0.69 | 0.64 | 0.64 |
| Concept Mixing | CLIPScore (Hessel et al., 2021) | 0.62 | 0.24 | 0.25 |
| | DSGScore (Cho et al., 2024) | 0.42 | 0.25 | 0.18 |
| | VIEScore (Ku et al., 2024) | 0.52 | 0.16 | 0.28 |
| | VQAscore (Lin et al., 2024) | 0.67 | 0.52 | 0.48 |
| | Ours | 0.83 | 0.91 | 0.87 |
| Numerical | CLIPScore (Hessel et al., 2021) | 0.61 | 0.22 | 0.16 |
| | DSGScore (Cho et al., 2024) | 0.47 | 0.21 | 0.29 |
| | VIEScore (Ku et al., 2024) | 0.87 | 0.74 | 0.68 |
| | VQAscore (Lin et al., 2024) | 0.78 | 0.64 | 0.57 |
| | Ours | 0.65 | 0.67 | 0.62 |
| Mathematical | CLIPScore (Hessel et al., 2021) | 0.72 | 0.44 | 0.54 |
| | DSGScore (Cho et al., 2024) | 0.60 | 0.45 | 0.43 |
| | VIEScore (Ku et al., 2024) | 0.72 | 0.44 | 0.46 |
| | VQAscore (Lin et al., 2024) | 0.63 | 0.33 | 0.67 |
| | Ours | 0.69 | 0.93 | 0.87 |
| Average | CLIPScore (Hessel et al., 2021) | 0.631 | 0.263 | 0.310 |
| | DSGScore (Cho et al., 2024) | 0.520 | 0.220 | 0.254 |
| | VIEScore (Ku et al., 2024) | 0.694 | 0.494 | 0.451 |
| | VQAscore (Lin et al., 2024) | 0.629 | 0.463 | 0.563 |
| | Ours | 0.713 | 0.747 | 0.694 |

Figure 12: **Examples of Seven Subfields in Commonsense Reasoning**, spanning Affordance, Attribute, Color, Emotion Intention Commonsense, Social Cultural Knowledge Object and Scene and Temporal Understanding. We showcase the Text-lite version.

Figure 13: **Examples of Seven Subfields in Logical Reasoning**, spanning Abductive, Categorical, conjunctive, Deductive, Hypothetical, Sufficient Conditional.

Figure 14: **Examples of Eight Subfields in Mathematical Reasoning**, spanning Combinatorial, Crypographic Encoding, Geometrical Transformations, Mathematical Function,spatial reasoning,et Theory, Spatial Reasoning and Vector Matrix Visualizations.

Figure 15: **Examples of Two Subfields in Concept Mixing**, including Functional Mixing and Literal Mixing.



Figure 16: **Examples of Three Subfields in Compositional Reasoning**, including Creative Compositional, Inferential Spatial, Color, Prescriptive Spatial.

Figure 17: **Examples of two Subfields in Causal Reasoning**, including Cause to Effect Reasoning and Cause to Effect Reasoning.



Figure 18: **Examples of Three Subfields in Numerical Reasoning**, including Approximate Number Generation, Conceptual Quantitative, Exact Number Generation.

| Model | Size | Overall | Commonsense | Compositional | Con.Mix | Logical | Numerical | Mathematical | Causal |
|-------|------|---------|-------------|---------------|---------|---------|-----------|--------------|--------|
| Nano-Bbanana | - | 0.67 | 0.69 | 0.70 | 0.79 | 0.71 | 0.69 | 0.23 | 0.67 |
| DALL-E-3 | - | 0.71 | 0.78 | 0.76 | 0.86 | 0.69 | 0.69 | 0.21 | 0.64 |
| GPT-Image-1 | - | 0.77 | 0.83 | 0.87 | 0.89 | 0.81 | 0.88 | 0.58 | 0.71 |

Table 22: **Comparative Performance of `Nano-Banana` and Other Proprietary Models** on `R2I-Bench`



Figure 19: **Qualitative Analysis of `Nano-Banana` on `R2I-Bench`**